Bio-Inspired Self-Cleaning Surfaces

Kesong Liu[1] and Lei Jiang[1,2]

[1]Key Laboratory of Bio-Inspired Smart Interfacial Science and Technology of Ministry of Education, School of Chemistry and Environment, Beihang University, Beijing 100191, PR China; email: liuks@buaa.edu.cn

[2]Beijing National Laboratory for Molecular Sciences (BNLMS), Key Laboratory of Organic Solids, Institute of Chemistry, Chinese Academy of Sciences, Beijing 100190, PR China; email: jianglei@iccas.ac.cn

Annu. Rev. Mater. Res. 2012. 42:231–63

First published online as a Review in Advance on May 29, 2012

The *Annual Review of Materials Research* is online at matsci.annualreviews.org

This article's doi: 10.1146/annurev-matsci-070511-155046

1531-7331/12/0804-0231$20.00

Keywords

anti-icing, antifogging, antireflection, drag reduction, superhydrophilicity, superhydrophobicity

Abstract

Self-cleaning surfaces have drawn a lot of interest for both fundamental research and practical applications. This review focuses on the recent progress in mechanism, preparation, and application of self-cleaning surfaces. To date, self-cleaning has been demonstrated by the following four conceptual approaches: (*a*) TiO_2-based superhydrophilic self-cleaning, (*b*) lotus effect self-cleaning (superhydrophobicity with a small sliding angle), (*c*) gecko setae–inspired self-cleaning, and (*d*) underwater organisms–inspired antifouling self-cleaning. Although a number of self-cleaning products have been commercialized, the remaining challenges and future outlook of self-cleaning surfaces are also briefly addressed. Through evolution, nature, which has long been a source of inspiration for scientists and engineers, has arrived at what is optimal. We hope this review will stimulate interdisciplinary collaboration among material science, chemistry, biology, physics, nanoscience, engineering, etc., which is essential for the rational design and reproducible construction of bio-inspired multifunctional self-cleaning surfaces in practical applications.

INTRODUCTION

Self-cleaning is a desired property for human beings and makes the dream of a contamination-free surface come true (1–5). Research on self-cleaning surfaces has not only fundamental interest but a wide domain of promising practical applications in daily life, industry, agriculture, and the military (6–9). The story of natural self-cleaning surfaces begins with the sacred lotus (*Nelumbo nucifera*), which has been a symbol of purity in Asia for more than 2,000 years. During the past few decades, many different synthesis strategies have been developed to design and fabricate self-cleaning surfaces (10–13). Today, a great variety of self-cleaning surfaces have also been commercialized. According to the mechanism of self-cleaning, these synthesis strategies can be classified into the following four categories: (*a*) TiO_2-based self-cleaning arising from photocatalysis and photo-induced superhydrophilicity, (*b*) lotus effect self-cleaning (superhydrophobicity with a small sliding angle) in which dirt particles on low-adhesive superhydrophobic surfaces can be easily removed by water droplets, (*c*) gecko setae–inspired, dry self-cleaning in which particulate contamination is cleaned solely by contact with a dry surface without using water droplets or other liquid, and (*d*) underwater organisms (shark skin, pilot whale skin, carp scale, etc.)–inspired, antifouling self-cleaning in which underwater biofouling organisms cannot settle and grow on bio-inspired antifouling surfaces with special chemical and physical structures.

This review focuses on recent developments in the mechanism, fabrication, and application of self-cleaning surfaces. The majority is organized into four sections. First, a brief summary of fundamental theories relevant to self-cleaning is presented. Second, we focus on the approaches to self-cleaning surfaces, with particular focus on TiO_2-based, lotus effect–inspired, gecko foot–inspired, and underwater organisms–inspired self-cleaning surfaces. Third, practical applications of self-cleaning surfaces in antifogging, anti-icing, antireflection, corrosion resistance, drag reduction, exterior construction materials, sensor, solar cell, textiles, and other fields are described. Finally, the remaining challenges and future outlook of self-cleaning surfaces are briefly addressed. Given space constraints, we could not review all the significant and interesting work in this active field.

FUNDAMENTAL THEORIES

Typical Wetting Models

The wetting behavior of solid surfaces by a liquid is a classical and important aspect of surface science. In 1805, Young (14) was the first to describe the basic law determining the equilibrium shape of a liquid drop on a surface. For a liquid droplet on an ideal flat film, wettability is determined by the surface free energy of solid substrates. The well-regarded Young's equation gives the following relation: $\gamma_{sg} = \gamma_{sl} + \gamma_{lg}\cos\theta_Y$, where θ_Y is Young's contact angle and γ_{sg}, γ_{sl}, and γ_{lg} refer to the interfacial surface tensions of solid, liquid, and gas, respectively. Young's angle is an ideal result of thermodynamic equilibrium of free energy at the solid-liquid-gas interface, where the influences of roughness, chemical heterogeneity, and others are neglected. In fact, solid surfaces are far from this ideal situation. Surface roughness is now thought to be an important parameter controlling surface contact angles and should be considered during the evaluation of surface wettability. Two wetting models are commonly employed to correlate surface roughness with the apparent contact angle: the Wenzel and Cassie-Baxter models.

In 1936, Wenzel (15) described a model to clarify the relationship between surface roughness and contact angle by the following equation: $\cos\theta_W = r\cos\theta_Y$, where θ_W is the apparent contact angle in the Wenzel model, θ_Y is Young's contact angle, and r is the surface roughness factor

given by the ratio of rough to planar surface areas. The Wenzel model predicts that surface roughness enhances wettability depending on the nature of the corresponding flat surface (1). If r is greater than 1, a hydrophobic surface ($\theta_Y > 90°$) becomes more hydrophobic ($\theta_W > \theta_Y$) when rough, whereas a hydrophilic surface ($\theta_Y < 90°$) shows increased hydrophilicity ($\theta_W < \theta_Y$). Although these tendencies are generally (but not always) observed, the Wenzel model is not sufficient when one is dealing with a heterogeneous surface.

In 1944, Cassie & Baxter (16) derived an equation to describe the effect of chemical heterogeneities on the contact angle of solid surfaces. If only air is present between the solid and the liquid, the cosine of the contact angle is −1; in this case, the Cassie-Baxter equation can be described as: $\cos\theta_{CB} = f_s(\cos\theta_Y + 1) - 1$, where θ_{CB} is the apparent contact angle in the Cassie-Baxter model and f_s is the surface fraction of the solid. The Cassie-Baxter equation was found to be useful in estimating the contact angle of heterogeneous surfaces.

In addition to the above-mentioned wetting models, other models have recently been proposed by investigating the coexistence and transition between the Wenzel and Cassie-Baxter states (17–19). These newer wetting models provide an avenue for the design of functional surfaces with special wettability. On the basis of these principles, intensive studies have been conducted to realize special functional surfaces with self-cleaning properties.

Superhydrophilicity-Induced Self-Cleaning

Superhydrophilicity is an important property of surfaces that can endow materials with self-cleaning ability. Water droplets can spread out and form a thin film on superhydrophilic surfaces. When rain or a light spray of water flows onto such surfaces, it can wedge into the space between the substrate and any dust that is present, washing the dust away.

Among the wide variety of superhydrophilic materials, titania (TiO_2) is one of the most promising. Since the first discovery of a light-induced amphiphilic (both hydrophilic and oleophilic) TiO_2 surface by Fujishima et al. (20) in 1997, TiO_2 has been widely used for hydrophilic-induced self-cleaning surfaces due to its favorable physical and chemical properties. TiO_2 can exhibit photocatalytic and photo-induced superhydrophilic properties. Although the self-cleaning mechanisms of TiO_2 have been extensively investigated over the past decade, further research continues to clarify the exact mechanism for the destruction of specific pollutants (9). The basic model for the self-cleaning mechanism of TiO_2 can be summarized as follows. The band gap of bulk anatase TiO_2 is 3.2 eV, corresponding to light of wavelength 390 nm, which is near-UV light. When a TiO_2 film is irradiated under UV light, excited charge carriers (i.e., electrons and holes) are generated on the surface of the film (**Figure 1**). Photogenerated holes decompose adsorbed organic dust molecules while electrons combine with atmospheric oxygen to produce the superoxide radical, which quickly attacks nearby organic molecules. During the photocatalytic reaction, the TiO_2 photocatalyst decomposes organic contamination through absorbing light with energy equal to or greater than its band gap energy and keeps the surface clean. In addition to its photocatalytic property, TiO_2 possesses another property—i.e., photo-induced superhydrophilicity. UV irradiation results in the formation of oxygen vacancies on the TiO_2 surface. These oxygen vacancies render the surface favorable for the adsorption of dissociative water, and surface hydroxide groups are produced. Thus, under UV irradiation, TiO_2 surfaces become progressively superhydrophilic (21). Water droplets can spread out and, if the substrate is glass, become transparent, which is the basis for antifogging coatings. The cooperation of photocatalysis and photo-induced superhydrophilicity on TiO_2 surfaces results in the desired self-cleaning function, which endows TiO_2 with a wide variety of practical applications.

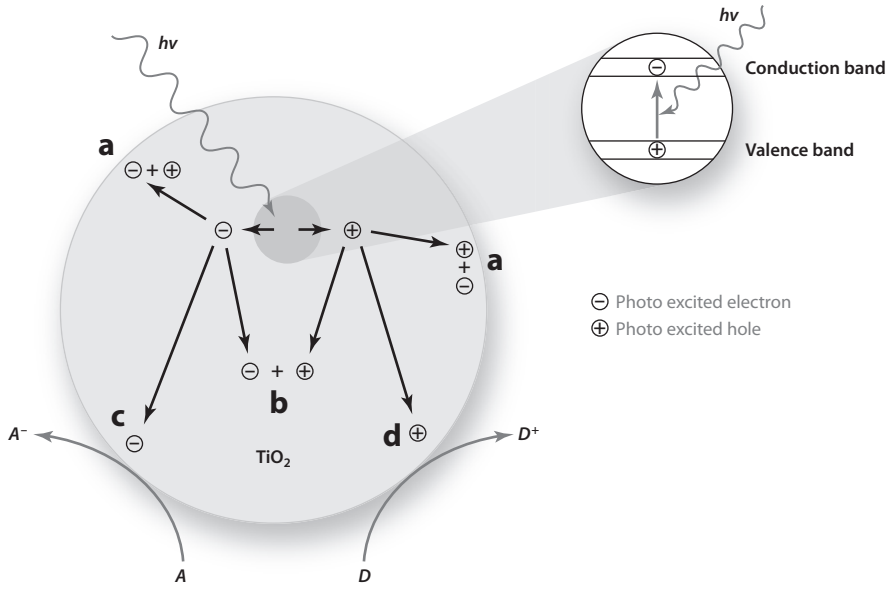

Figure 1

Upon irradiation of TiO_2 by ultra-band gap light, the semiconductor undergoes photoexcitation. The electron and the hole that result can follow one of several pathways: (*a*) electron-hole recombination on the surface, (*b*) electron-hole recombination in the bulk reaction of the semiconductor, (*c*) electron acceptor A reduction by photogenerated electrons, or (*d*) electron donor D oxidization by photogenerated holes (8).

Superhydrophobicity-Induced Self-Cleaning

In the preceding section, the mechanism of superhydrophilicity-induced self-cleaning was presented. This section focuses on the mechanism of superhydrophobicity-induced self-cleaning, with particular emphasis on the lotus effect.

After billions of years of evolution, some biological materials possess excellent surface wettability and exhibit a superhydrophobicity-induced self-cleaning property (2–5, 11). Among the variety of self-cleaning biomaterials, the lotus (*Nelumbo nucifera*) leaf, better known as the water lily, is one of the most promising. In Asia, the lotus has been a symbol of purity in religions and cultures for more than 2,000 years due to its self-cleaning nature. Lotus roots are embedded in muck, but the plant's leaves are seemingly never dirty. Water droplets falling onto the leaves bead up and roll off. Rainwater washes dirt from the lotus leaves so that they are self-cleaning, which is the so-called lotus effect.

Although the self-cleaning property of the lotus has been recognized in Asia for more than 2,000 years, the mechanism has been explored by scientists only since the early 1970s, after the introduction of the scanning electron microscope (SEM). Since then, a great number of studies have been conducted to unravel the self-cleaning mechanism of lotus leaves (22, 23). Research has indicated that lotus leaf surfaces possess randomly distributed micropapillae with diameters ranging from 5 μm to 9 μm (**Figure 2*a***). On every papilla, fine branch-like nanostructures with diameter of approximately 120 nm have been observed (**Figure 2*b***). Multiscale structures provide air pocket formation, resulting in the lowest contact area between lotus leaf surfaces and water droplets. Furthermore, hydrophobic three-dimensional (3D) epicuticular waxes with a tubule structure have also been found on lotus leaf surfaces (**Figure 2*c***) (3–5). The cooperation of surface

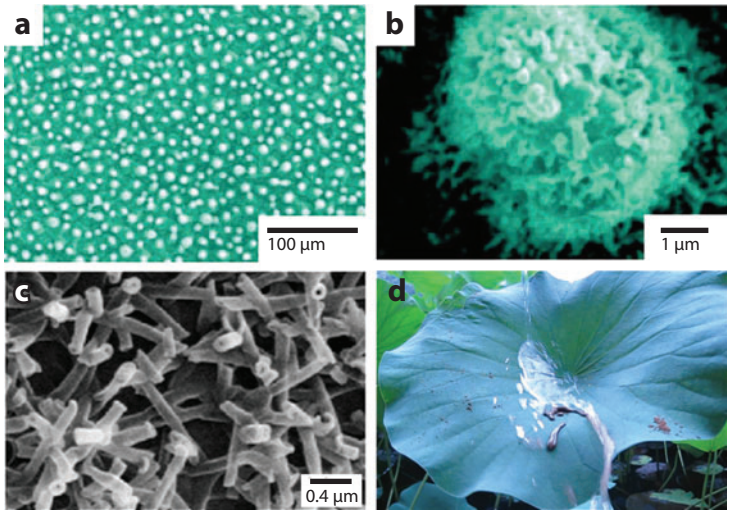

Figure 2

(*a*) Large-area SEM image of the lotus leaf surface (23). Every epidermal cell forms a papilla and has a dense layer of epicuticular waxes superimposed on it. (*b*) Enlarged view of a single papilla from panel *a*. (*c*) SEM image of 3D epicuticular wax tubules on lotus leaf surfaces, which create nanostructures (3–5). (*d*) Water droplets roll easily across the lotus leaf surface and pick up dirt particles, demonstrating the self-cleaning effect.

micronanoscale hierarchical structures and hydrophobic epicuticular waxes confers a high water contact angle and a small sliding angle, exhibiting superhydrophobic and low-adhesion characteristics. The water contact angle and sliding angle of lotus leaves are approximately 160° and 2°, respectively. Water droplets on their surface are almost spherical and can roll freely in all directions and then pick up dirt particles (**Figure 2*d***). A very high static water contact angle and a very low sliding angle are essential for achieving superhydrophobicity-induced self-cleaning. Similar superhydrophobic self-cleaning properties can also be found in lady's mantle leaves, taro leaves, cicada wings, termite wings, and other biological materials (2–5, 24).

Others

The mechanisms of TiO_2-based superhydrophilic self-cleaning and lotus effect superhydrophobic self-cleaning are presented above. Gecko setae, shark skin, pilot whale skin, carp scale, and other biomaterials have also demonstrated self-cleaning properties, although they achieve this characteristic differently than do TiO_2 and lotus leaves. The self-cleaning mechanism of gecko setae, shark skin, pilot whale skin, and carp scale, as well as the corresponding bio-inspired self-cleaning surfaces, are discussed in the following section.

APPROACHES TO SELF-CLEANING SURFACES

TiO_2-Based Superhydrophilic Self-Cleaning Surfaces

Due to TiO_2's special photo-induced properties—photocatalysis and photo-induced superhydrophilicity—a wide variety of TiO_2-based superhydrophilic self-cleaning surfaces have

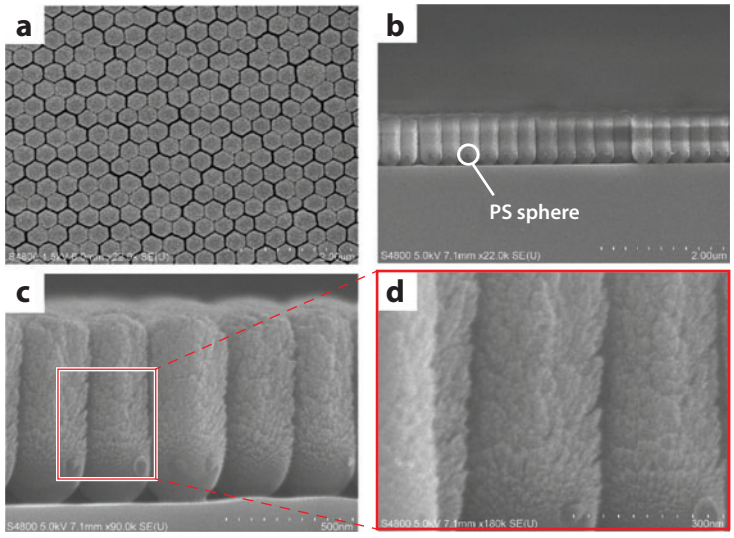

Figure 3

SEM images of a sample obtained by pulsed laser deposition using a polystyrene colloidal monolayer as the substrate. (*a*,*b*) Low-magnification images observed from the top and side. (*c*,*d*) High-resolution images observed from the side. Panel *d* is an expanded image of panel *c* (29).

been fabricated using different synthesis approaches on different substrates (6–9, 25–28). Through the use of polystyrene colloidal monolayers as templates (29), a hierarchical amorphous TiO_2 nanocolumn array was fabricated by pulsed laser deposition (**Figure 3**). The hexagonal-close-packed nanocolumn array presented superamphiphilicity with both water and oil contact angles of 0° without UV irradiation. Interestingly, amorphous TiO_2 arrays exhibited superior photocatalytic performance relative to anatase nanocolumn arrays due to large surface area and special microstructures. The combination of superamphiphilicity and photocatalytic activity endowed the surface with a self-cleaning property. In addition to TiO_2, similar nanocolumn arrays of other materials, including SnO_2, Fe_2O_3, and carbon, can also be fabricated by using this strategy and then transferred to almost any substrate. Daoud et al. (30) reported the fabrication of self-cleaning keratin fibers through bottom-up nanotechnology. To introduce additional carboxylic groups, fibrous proteins were modified with succinic anhydride, resulting in enhanced bonding between TiO_2 and the fibers and more effective self-cleaning properties.

In the past few years, mesoporous materials (pore size between 2 and 50 nm) have attracted much attention because of their potential applications in large-molecule separation, catalysis, medical implants, energy conversion, membranes, and optical fields (31–34). Transparent mesoporous TiO_2-SiO_2 nanocomposite films with self-cleaning ability were prepared by Allain et al. (35) through the dispersion of colloidal TiO_2 nanoparticles in a sol-gel mesoporous silica binder. The quantum-yield efficiency was approximately 1.1%, and the photocatalytic efficiency of the mesoporous TiO_2-SiO_2 films was approximately 15 times higher than that of microporous films. This can be attributed to a closer contact between the organic molecules and particle surfaces and the improved diffusion rate of water and oxygen through the interconnected pore network. Recently, Fateh et al. (36) fabricated highly active crystalline mesoporous TiO_2 films precoated with SiO_2 for self-cleaning applications. The obtained transparent coatings presented high photonic efficiency ($\zeta = 0.078\%$).

Table 1 Typical lotus effect–inspired self-cleaning materials fabricated using different approaches[a]

Material	Method	Structure	Reference
Al	Self-assembly	Concave-like	51
BMG	Chemical etching	Coral-like	41
Boron nitride	B ink	Nanotube	52
Boron nitride	CVD	Nanosheet	53
Cellulose	ATRP	Graft-on-graft	39
CNT	CVD	Hierarchical	54
CNT	CVD	Vertical array	55
ETPTA	Bottom-up	Macroporous	56
MWCNTs	Casting process	Honeycomb	57
MWCNT/PDMS	Spin coating	Hierarchical	50
MWCNT/silane sol	Spray coating	Porous	58
PDMS	Lithography	Inverse-trapezoidal	59
Peptide	Self-assembly	Nanowire	60
PMMA	Electron irradiation	Microspheres	61
Polysiloxane/TiO_2	Spraying	Hierarchical	62
Poly(SiMA-*co*-MMA)	Spray deposition	Lotus leaf–like	63
Sb_2O_3	Hydrothermal	Hierarchical	48
SiC	Vapor-solid reaction	Nanowire	64
Silica	Colloid assembly	Hierarchical	65
Silicon wafer	Chemical etching	Pyramidal	42
ZnO/CuO	Hydrothermal	Nanotree array	49

[a]Abbreviations: ATRP, atom transfer radical polymerization; CNT, carbon nanotube; CVD, chemical vapor deposition; ETPTA, ethoxylated trimethylolpropane triacrylate monomer; MMA, methylmethacrylate; MWCNTs, multiwalled carbon nanotubes; PCC, precipitated calcium carbonate; PDMS, poly(dimethylsiloxane); PMMA, poly(methyl methacrylate); SiMA, 3-{tris[(trimethylsilyl)oxy]-silyl}propylmethacrylate.

Lotus Effect–Inspired Self-Cleaning Surfaces

The multiscale structured surface of the lotus leaf provided a model for the construction of biomimetic self-cleaning surfaces. Bhushan et al. (37) investigated the wettability, adhesion properties, and self-cleaning efficiency of flat hydrophilic and hydrophobic, nanostructured, microstructured, and multiscale-structured superhydrophobic surfaces. They found that geometric scale effects contributed to superior self-cleaning performance of nanostructured surfaces. To date, inspired by lotus leaves, many different synthesis strategies have been developed to fabricate superhydrophobic self-cleaning surfaces. Some typical lotus effect–inspired self-cleaning surfaces are summarized in **Table 1**.

Atom transfer radical polymerization. In recent years, atom transfer radical polymerization (ATRP) has proved useful and become the widely employed technique for the synthesis of functional macromolecules with controlled and complex architectures. Superhydrophobic self-cleaning cellulose surfaces with multiscale structures have been fabricated through the combination of ATRP of glycidyl methacrylate followed by pentadecafluorooctanoyl modification (38). After contamination of the surface with carbon black powder, water droplets adsorbed the dirt and rolled off the surface when the substrate was tilted. ATRP is also useful for the construction of

superhydrophobic and self-cleaning cellulose surfaces without any fluorine-containing compound modification (39). The environmentally friendly approach using nonfluorinated compounds remains a challenge in the field of self-cleaning and related surface modification.

Chemical etching. Kim et al. (40) fabricated superamphiphobic (both superhydrophobic and superoleophobic) silicon surfaces on a large area (4-inch wafer) through a wet chemical etching method followed by a fluorinated self-assembled monolayer modification. Sticky dirt could be removed by glycerin droplets, confirming a superior self-cleaning capability. The superamphiphobic surface could be turned superamphiphilic by simply exposing the desired part(s) to UV light. A superamphiphobic CaLi-based bulk metallic glass surface was also constructed by Zhao et al. (41) through etching the surface with water and postmodification with a fluoroalkylsilane coating. Wafer-scale self-cleaning antireflective silicon surfaces with pyramidal hierarchical structures were prepared by employing potassium hydroxide etching and silver catalytic etching on a crystalline silicon wafer (42). Furthermore, through the use of the obtained hierarchical structures as templates, flexible superhydrophobic surfaces can be fabricated by imprint lithography. Robust superhydrophobic surfaces are of great importance for self-cleaning applications. Xiu et al. (43) demonstrated mechanically robust superhydrophobicity on hierarchically structured silicon surfaces. Unlike the polymeric and nanostructure-only surfaces, the hierarchical structures maintained their superhydrophobicity even after mechanical abrasion.

Chemical vapor deposition. Ultralyophobic (highly hydrophobic and oleophobic) oxidized aluminum surfaces exhibiting negligible contact angle hysteresis for water and *n*-hexadecane were prepared using the chemical vapor deposition (CVD) approach (44). CVD-produced organic molecule monolayers were expected to randomly immobilize covalently with respect to the oxidized aluminum surface. Owing to the topological effect of this monolayer, probe liquids hardly penetrated the monolayer to interact with residual aluminols on the surface, resulting in negligible contact angle hysteresis.

Electrospinning. Electrospinning is a simple but versatile method to generate continuous fibers with diameters as small as a few nanometers. Jiang et al. (45) fabricated a lotus leaf–like superhydrophobic polystyrene film with a composite structure consisting of porous microspheres and nanofibers (**Figure 4**). The porous microspheres contributed to the superhydrophobicity by increasing surface roughness, while nanofibers interwove to form a 3D network that reinforced the composite film. Furthermore, by adjusting the concentration of the starting solution, one could easily control the morphologies of the resultant materials. Asmatulu et al. (46) demonstrated superhydrophobic self-cleaning nanocomposite fibers using an electrospinning process. TiO_2 nanoparticles and graphene nanoflakes were incorporated into the electrospun fibers to induce superhydrophobicity. The tunable properties of TiO_2- and graphene-based superhydrophobic surfaces and electrodes could improve the efficiency of dye-sensitized solar cells. Inspired by the self-cleaning lotus leaf and silver ragwort leaf, biomimetic superhydrophobic surfaces were prepared by Lin et al. (47) through electrospinning polystyrene solution in the presence of silica nanoparticles. Owing to rapid phase separation during electrospinning, the resultant electrospun fiber surfaces were composed of nanoprotrusions and numerous grooves.

Hydrothermal approach. Utilizing antimony isopropoxide as the inorganic precursor and hexadecylamine as the structure-directing agent, Liu et al. (48) fabricated superhydrophobic Sb_2O_3 films using a hydrothermal approach without further modification (**Figure 5*a***). These superhydrophobic films with multiscale structures demonstrated a small sliding angle. Guo et al. (49)

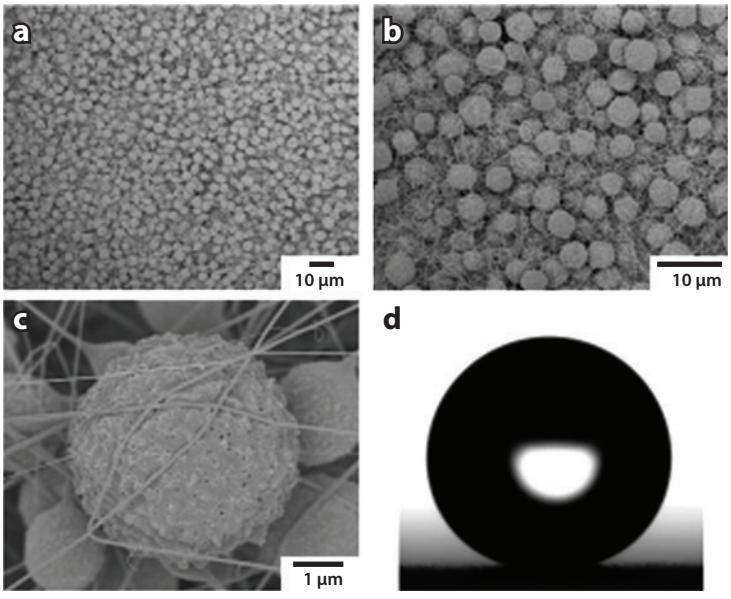

Figure 4

(*a*) SEM image of a porous microsphere/nanofiber composite film prepared using the electrospinning approach. (*b*) 3D network structure of the polystyrene composite film. (*c*) Surface nanostructure of a single porous microsphere. (*d*) A water droplet on the polystyrene composite film, exhibiting superhydrophilicity (45).

reported the fabrication of ZnO/CuO heterohierarchical nanotree arrays through a hydrothermal method combined with thermal oxidation (**Figure 5*b***). The secondary growth of ZnO nanorods enclosed with CuO nanowires, resulting in the formation of ZnO/CuO heterohierarchical nanotree arrays. After silanization, these nanotree arrays exhibited superhydrophobicity with a low contact angle hysteresis of almost 0°.

Spin coating. Wang et al. (50) demonstrated the fabrication of superhydrophobic flexible multiwalled carbon nanotubes/poly(dimethylsiloxane) (MWCNT/PDMS) films. The obtained

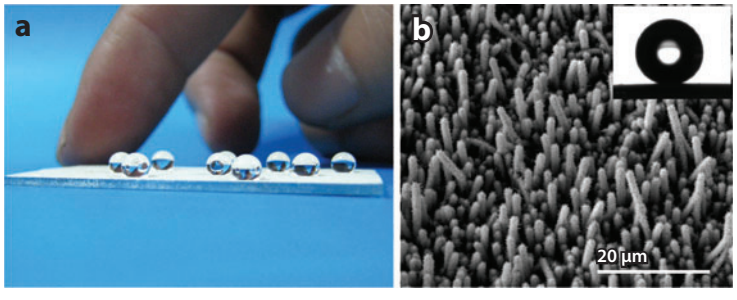

Figure 5

(*a*) Optical image of water droplets of different sizes (17–22 μl) on the as-synthesized Sb_2O_3 film surface, exhibiting superhydrophobicity (48). (*b*) SEM image of ZnO/CuO heterohierarchical nanotree arrays prepared via the hydrothermal approach. The inset is a water droplet profile on a ZnO/CuO array surface, demonstrating superhydrophobicity (49).

MWCNT/PDMS films maintained their superhydrophobicity after bending and pressing, exhibiting environmental stability. Furthermore, these superhydrophobic films could be coated onto glass, metals, and polymers, demonstrating water-repellent, self-cleaning surfaces with high water contact angles and low sliding angles. The MWCNT/PDMS films remained stable for two weeks under outdoor conditions when loaded on the roof of a car, with nearly no changes in their superhydrophobic and self-cleaning properties.

Gecko Foot–Inspired Self-Cleaning Surfaces

In the fourth century B.C., Aristotle observed the ability of the gecko to "run up and down a tree in any way, even with the head downwards" (66, 67). The gecko is an amazing animal and has evolved one of the most effective adhesives known in nature. The gecko foot is made up of well-aligned fine microscopic hairs called setae (approximately 110 μm in length and 5 μm in diameter), which are split into hundreds of smaller nanoscale ends called spatulae (68). Contact between the gecko spatulae and an opposing solid surface generates van der Waals forces that are sufficient to allow geckos to climb vertical walls or across ceilings. The van der Waals mechanism implies that gecko adhesion depends more on surface geometry than on surface chemistry (66, 67). Besides their remarkable adhesion, gecko feet also exhibit superhydrophobic and self-cleaning properties (66, 67, 69). Inspired by gecko feet, a variety of synthesis strategies have been applied to construct gecko-mimetic self-cleaning adhesives, including dry self-cleaning with solid surfaces and wet self-cleaning with water droplets.

Self-cleaning mechanism of gecko feet. Gecko setae are the first known self-cleaning adhesive in nature. In 2005, Hansen et al. (69) revealed how geckos manage to keep their feet clean while walking about with sticky toes. Different from the above-mentioned TiO_2 and lotus leaves, self-cleaning is a property intrinsic to nanostructured setal. Tokay gecko feet contaminated with microspheres could recover their ability to cling to vertical surfaces after only a few steps on clean glass. Similarly, isolated setal arrays self-cleaned by repeated contact with a clean surface. Contact mechanical models indicated that self-cleaning occurs by an energetic disequilibrium between the adhesive forces attracting a dirt particle to the substrate and those attracting the same particle to one or more spatulae (**Figure 6**). The researchers proposed that setal self-cleaning is dependent largely on particle and spatula size and spatula material properties. To rationally design dry self-cleaning adhesive nanostructures, an array of spatulae should have the following properties: (*a*) surface area smaller than that of dirt particles, (*b*) a composition of relatively hard, nontacky materials, and (*c*) low surface energy.

Gecko-inspired dry self-cleaning. Inspired by geckos, gecko-like high–aspect-ratio polypropylene microfibrillar adhesives possessing self-cleaning during contact were first fabricated by Lee et al. (70) in 2008 (**Figure 7**). In contrast to the conventional pressure-sensitive adhesive (PSA), the contaminated gecko-like stiff polypropylene fibrillar adhesive recovered 25–33% of the original shear adhesion force after multiple contacts (approximately 30 simulated steps) with a dry clean surface, demonstrating the dry self-cleaning property with microspheres (radius $\leq$2.5 μm). However, the synthetic microfibrillar adhesives could not self-clean larger particles, which is consistent with the Johnson-Kendall-Roberts pull-off force model. In addition to dry self-cleaning, these gecko-like adhesives also presented superhydrophobicity and wet self-cleaning with water droplets. Inspired by the remarkable self-cleaning properties of gecko feet, lotus leaves, and lady's mantle leaves, Sethi et al. (71) prepared carbon nanotube–based synthetic adhesives possessing superhydrophobicity, self-cleaning ability, and high shear resistance through optimizing length and

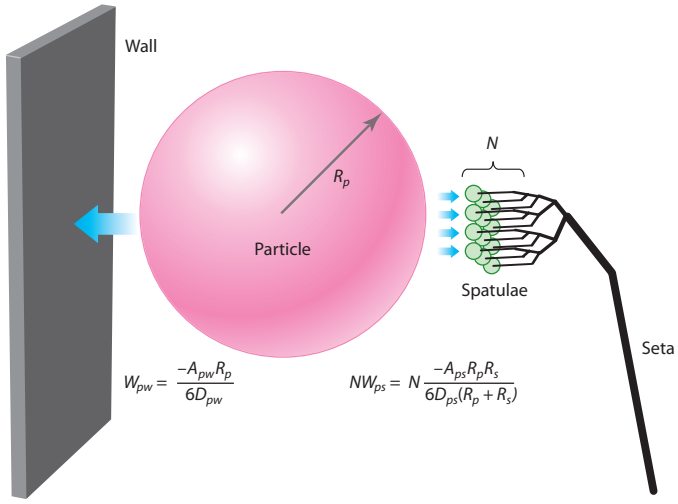

Figure 6

Model of interactions between N (number of particle-spatula interactions) gecko spatulae of radius R_s, a spherical dirt particle of radius R_p, and a planar wall. Van der Waals interaction energies for the particle-spatula (W_{ps}) and particle-wall (W_{pw}) systems are shown. When $N \times W_{ps} = W_{pw}$, equal energy is required to detach the particle from wall or N spatulae. N is sufficiently great that self-cleaning results from energetic disequilibrium between the wall and the relatively few spatulae that can attach to a single particle (69).

pattern size. The synthetic tapes could be cleaned by contact mechanics, similar to the procedure used for gecko feet (69). After a couple of contacts with mica (or glass substrate), the majority of dirt particles (silica particles ranging from 1 to 100 μm in size) on the synthetic tapes could be cleaned. Only a few small silica particles remained stuck to the surface and in between the pillars of the carbon nanotube. Beyond their dry self-cleaning ability, the synthetic carbon nanotube–based

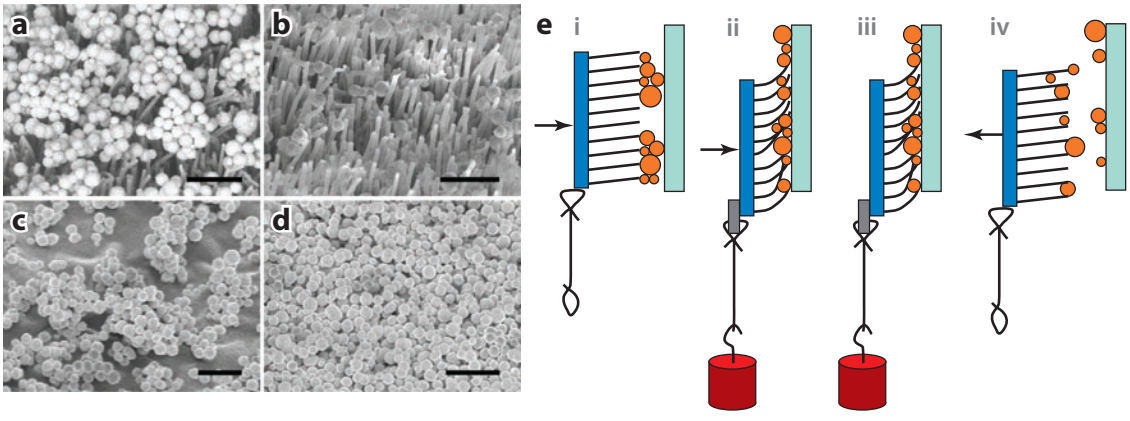

Figure 7

SEM images of polypropylene fibrillar adhesive and conventional PSA. (*a*) Fibrillar adhesive contaminated by gold microspheres. (*b*) Fibrillar adhesive after 30 contacts (simulated steps) on a clean glass substrate. (*c*) Conventional PSA contaminated by microspheres. (*d*) Conventional PSA after contact on a clean glass substrate. All scale bars correspond to 10 μm. Microspheres on fibrillar adhesive are removed by simulated steps, but microspheres on PSA cover more area after the steps. (*e*) One cycle of simulated steps, with contact with an initially clean glass slide. (*i*) Applying normal compressive force. (*ii*) Shear load added to the compressive load by a hanging weight. (*iii*) Removing the compressive load (pure shear loading). (*iv*) Detaching the sample (70).

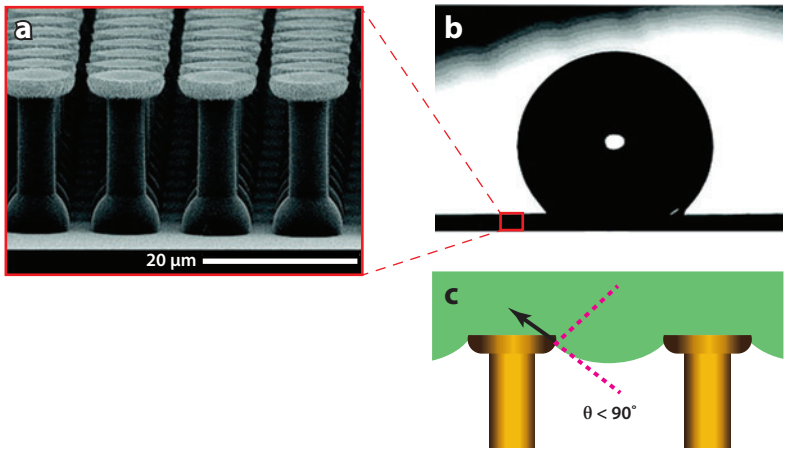

Figure 8

(*a*) SEM image of a polyurethane mushroom-shaped microfiber array with approximately 5 μm stem diameter, 9 μm tip diameter, and 20 μm length. (*b*) The optical microscopic profile view of a deionized water droplet on the fiber array. (*c*) Schematic diagram illustrating possible liquid-air interfaces on the fiber array (72).

gecko tapes could also be cleaned by water, mimicking the leaves of lotus and lady's mantle plants in nature. When rinsed with water, the water droplets rolled off very easily and picked up dirt particles along the way. After mechanical cleaning, the shear strength recovered back to 90% (and 60% for water-cleaned samples) of the values measured before soiling, which is superior to such strength recovery in geckos (69).

Gecko-inspired wet self-cleaning. Inspired by gecko feet and lotus leaves, mushroom-shaped microfibrillar adhesives were fabricated by Kim et al. (72) using a soft hydrophilic polyurethane elastomer (**Figure 8**). The mushroom-shaped microfiber arrays exhibited both wet self-cleaning and dry adhesion. Almost 100% of silica particles (5–50 μm in diameter) on the elastomer arrays were cleaned, similar to the lotus effect found in nature. Moreover, contaminated and then wet self-cleaned fiber arrays showed almost 100% adhesion recovery, i.e., without any degradation of adhesive strength. The remarkable wet self-cleaning ability could be attributed to the mushroom-shaped tip geometry of the fiber array. This research implies that rational design of tip shape is important for the fabrication of polymer fibrillar adhesives with self-cleaning ability. This design principle was further demonstrated by Haq et al. (73). A synthetic gecko tape with mushroom-shaped hairs was prepared through photolithographic and nanomolding methods. The obtained mushroom-shaped hairs exhibited superhydrophobicity and superior adhesion strength. Furthermore, simply washing with water recovered adhesion strength after contamination with dust and foreign hairs, showing wet self-cleaning. Mimicking the nanostructure of gecko foot hairs, Kustandi et al. (74) fabricated wafer-scale parylene nanofibrillar structures through a combination of nanolithography, etching, and nanomolding. The resultant polymer surface was composed of packed nanofibrils possessing superhydrophobic, water-repellent, and easy-to-clean characteristics. The synthetic nanostructured surface adhered firmly to a smooth glass substrate and exhibited a contaminant-free self-cleaning characteristic similar to that of gecko setal nanostructures. Importantly, the surface could be cleaned almost completely of particulate contaminants by either

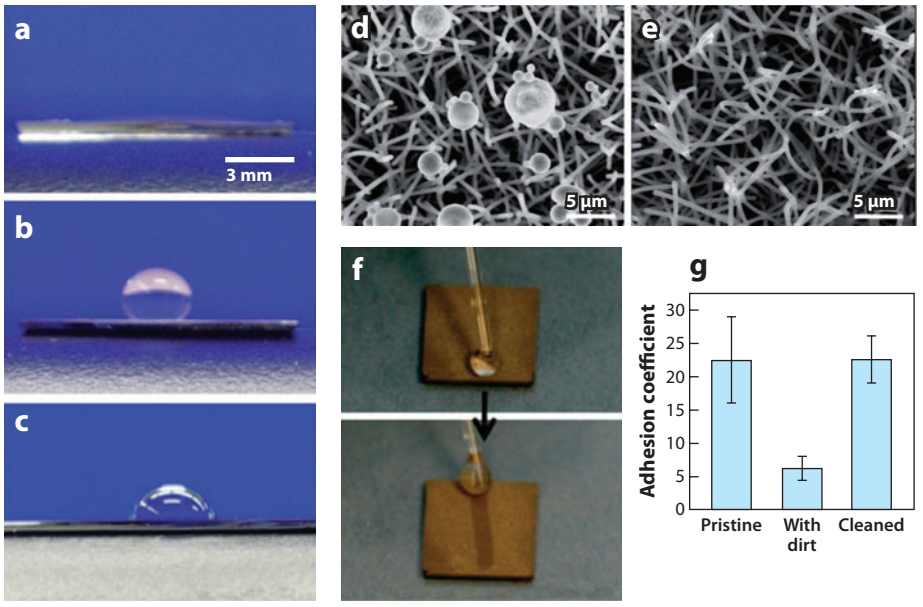

Figure 9

Wet self-cleaning of superhydrophobic nanowire connectors. Contact angle measurements for (*a*) pristine Ge nanowire arrays, (*b*) parylene coated Ge nanowire arrays, and (*c*) parylene coated Si substrate. The optical images illustrate a water droplet placed on the surface of each substrate. SEM images of nanowire forests (*d*) contaminated with alumina and silica particles (approximately 1–11 µm) and (*e*) cleaned with rolling a water droplet. (*f*) Wet self-cleaning procedure on surface-contaminated nanowire forests, in which a water droplet is gently rolled on the surface by a glass rod during which contaminants are efficiently removed from the surface by the lotus effect. (*g*) Comparison of the adhesion coefficient (shear-to-preload ratio) of pristine, contaminated, and cleaned nanowire connectors (75).

using a rolling water droplet or attaching wetted mica to the nanostructured surface, exhibiting wet self-cleaning.

The above-mentioned gecko-inspired dry or wet self-cleaning adhesives were used primarily in dry adhesion fields. Recently, Ko et al. (75) demonstrated self-cleaning Ge/parylene nanowire connectors that possessed both dry and wet (underwater) adhesion properties (**Figure 9**). The nanowire connectors bound strongly even under lubricating conditions, such as in the presence of mineral oil, due to their high aspect ratios. Adhesion strength, repeated reusability, and mechanical robustness of the nanowire connectors were strongly dependent on the geometric configuration of nanowire forests with an optimal length (approximately 10 µm). Hybrid nanowire connectors presented wet self-cleaning, similar to the lotus effect, where the contaminant particles on the surface were efficiently removed by rolling water droplets. These nanowire connectors nearly recovered their full shear adhesion strength, matching that of the neat state, after the wet self-cleaning process. This research provides an avenue for designing novel gecko-inspired self-cleaning adhesives for use in underwater conditions.

Underwater Organisms–Inspired Self-Cleaning Surfaces

In aquatic environments, fouling organisms adsorb and subsequently attach and grow on submerged surfaces. Biofouling is a widespread and serious problem for both aquatic organisms and

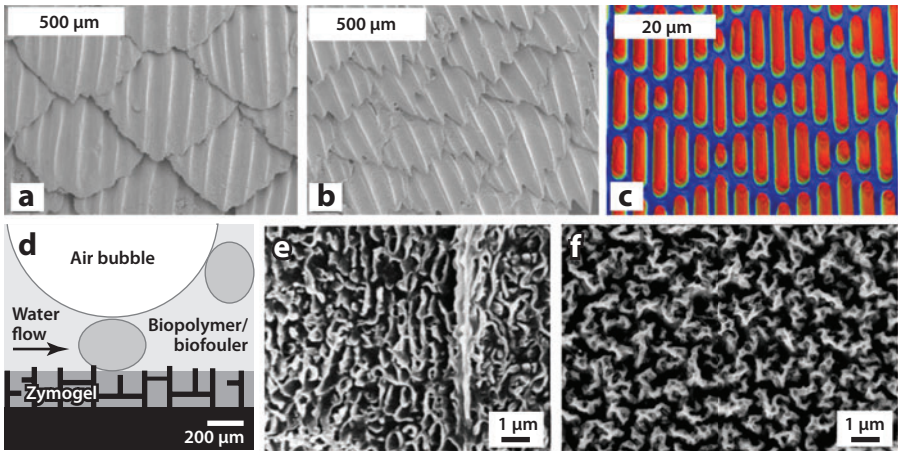

Figure 10

SEM images of (*a*) spinner shark skin and (*b*) Galápagos shark skin surfaces. (*c*) White-light optical profilometry image of Sharklet AF^{TM} (76). (*d*) Preliminary model of self-cleaning abilities of pilot whale (*Globicephala melas*) skin, based on the relief of nanoridges filled with a medium (82). (*e*) SEM image of the self-cleaning pilot whale skin. The pores enclosed by the nanoridges are displayed very clearly (82). (*f*) SEM image of pilot whale–inspired self-cleaning structures fabricated by polyelectrolyte self-assembly (84).

man-made underwater structures (76, 77). For example, biofouling results in large functional and monetary costs to both military and commercial vessels by increasing fuel costs due to drag, the cost of dry docking for cleaning, and loss of hull strength due to biocorrosion. Current antifouling agents (such as tributyltin and lead) usually have a negative impact on the environment. Therefore, the design and manufacture of universal, environmentally friendly coatings with both antifouling and fouling-release properties are still an enormous challenge.

After billions of years of evolution, nature provides many examples of mechanisms to control fouling. Underwater organs such as some shark skin, whale skin, carp scales, mollusks, gorgonian corals, and others possess natural antifouling defenses, resulting from the combination of special chemical and physical structures.

Shark skin. Shark skin can prevent marine organisms from being able to adhere to its surface, exhibiting self-cleaning. Shark skin is a more recent focus for biomimetic antifouling self-cleaning technologies, having been investigated initially for its drag reduction properties in aircraft design (78, 79). To date, a variety of shark skins have been investigated (**Figure 10*a*,*b***) because the number of ribs per scale and the length and spacing of the microtexture vary slightly between species (78). The unique skin structures and a mucosal coating secreted by epidermal cells not only prevent sea plants and organisms from adhering to it (self-cleaning), but also enable the shark to swim faster and more efficiently. Different from the above-mentioned TiO_2, lotus leaves, and gecko feet, the self-cleaning mechanism of shark skin with hydrophilicity can be attributed to the following considerations (80): (*a*) The accelerated water flow at a shark's surface reduces the contact time of fouling organisms; (*b*) the rough nanotexture on shark skins reduces the available surface area for organism adhesion; and (*c*) the dermal scales themselves perpetually realign or flex in response to changes in internal and external pressure as the shark moves through water, creating a moving target for fouling organisms. Inspired by shark skin, a variety of antifouling self-cleaning surfaces have been developed using different synthesis strategies (76). For example,

Carman et al. (81) demonstrated a nontoxic strategy for inhibiting the settlement of fouling organisms using poly(dimethylsiloxane) elastomer. The resultant bio-inspired surface topography, Sharklet AF™ (**Figure 10*c***), reduced the attachment of zoospores of *Ulva* by 86% compared with smooth elastomer.

Pilot whale skin. In addition to self-cleaning antifouling shark skin, pilot whale (*Globicephala melas*) skin also demonstrates a very clean surface free of all fouling organisms (82, 83), arising from nanoridge pores and zymogel on the skin surface (**Figure 10*d*,*e***). The pilot whale skin surface and the intercellular gel contain both polar and nonpolar functional groups, which contributes to short- and long-term fouling reduction (83). This special skin surface property, combined with the speed of movement, surfacing, and jumping, may contribute to removing weakly adhered epibionts. Extensive research on self-cleaning pilot whale skin provided an important inspiration for the design and construction of self-cleaning antifouling surfaces. For example, Cao et al. (84) recently fabricated pilot whale skin–like structures using layer-by-layer spray-coated multilayered polyelectrolytes (**Figure 10*f***). The settlement of zoospores of *Ulva* was strongly influenced by the size of the features present on the surfaces. The surface features at the same scale (on the order of 2 μm) as that for pilot whale skin showed the lowest settlement of *Ulva* regardless of surface chemistry.

Carp scales. Grass carp (*Ctenopharyngodon idella*) can freely swim and effectively resist oil pollution or biofouling underwater, demonstrating self-cleaning. For grass carp, the self-cleaning mechanism can be attributed to the cooperation of surface hydrophilic mucus and multiscale structures (85). Grass carp scales possess superoleophilicity in air and superoleophobicity in water. Inspired by self-cleaning fish scales, Liu et al. (85) demonstrated a low-adhesive superoleophobic interface with hierarchical structures via an oil/water/solid three-phase system. With an increase in surface roughness, the contact angle of oil droplets increased, and the adhesive force decreased significantly. To attain robust underwater superoleophobicity, Lin et al. (86) prepared hierarchical poly(*N*-isopropylacrylamide) (pNIPAm)-nanoclay hybrid hydrogels inspired by carp scales (**Figure 11**). The combination of rigid nanoclays and flexible macromolecules contributed to the stability of trapped water on hierarchical surfaces and resulted in robust low-adhesion superoleophobicity. Furthermore, the biocompatible hybrid hydrogels presented high compressive and tensile strength, which is crucial for self-cleaning applications underwater.

Others

Spiders can produce cobwebs with high strength-to-density ratios; these cobwebs exhibit self-cleaning and strong and releasable adhesion, similar to gecko setae. Pugno et al. (87) demonstrated the importance of hierarchy in the design of superhydrophobic, self-cleaning, and superadhesive materials. By mimicking the natural materials, it is feasible to fabricate futuristic self-cleaning, superadhesive, releasable hierarchical smart tissues, as well as large invisible cables, through carbon nanotube technology.

Importantly, in addition to mimicking the above-discussed natural antifouling materials, superhydrophobic surfaces can also be used to construct self-cleaning antifouling coatings through the following two approaches (88): (*a*) mirror imaging the lotus effect, in the sense of designing a surface that repels biological entities, and (*b*) designing a surface that minimizes the water-wetted area when submerged in water (by keeping an air film between the water and the surface).

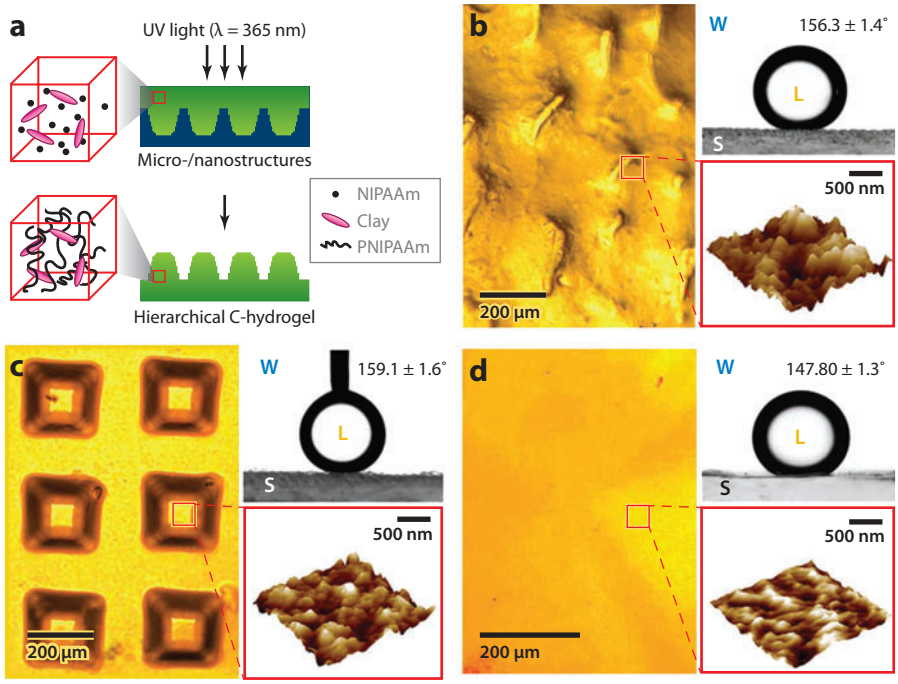

Figure 11

Bio-inspired strategy of constructing hierarchical hybrid hydrogels (86). (*a*) Schematic illustration of the mold method of fabricating hierarchical hybrid hydrogels through photo-initiated polymerization. (*b–d*) Optical and atomic force microscopy images of differently treated hydrogel surfaces. (*Top-right part of each panel*) Photographs of oil droplets (dichloroethane, 3 μl) on the different surfaces in water. (*b*) Micro/nanostructured surface of a fish-scale replica exhibits superoleophobicity. (*c*) Bio-inspired hierarchical surface with microprotuberances and nanometer-scale roughness shows superoleophobicity. (*d*) Nonpatterned smooth surface shows oleophobicity.

APPLICATIONS OF SELF-CLEANING SURFACES

Antifogging

Fogging is ubiquitous, as it frequently occurs on the surface of cold windshields, eyeglasses, safety glasses, and ski goggles. This problem can be effectively solved by controlling the interaction of liquids with surfaces. Recently, a number of synthesis strategies have been developed to fabricate self-cleaning antifogging surfaces. These synthesis strategies can be categorized following three principal approaches: (*a*) a superhydrophilic approach, (*b*) a superhydrophobic approach, and (*c*) a stimuli-responsive coating approach.

Superhydrophilicity-induced antifogging. Zorba et al. (89) demonstrated bio-inspired self-similar porous TiO_2 surfaces, presenting stable superhydrophilicity without UV light activation. Self-similar porous TiO_2 surfaces exhibited self-cleaning, antifogging, and high transmittance from near-UV to the infrared (**Figure 12*a***). Li et al. (90) presented the preparation of biomimetic superhydrophilic surfaces with antifogging and antireflective properties on silica substrates. These surfaces presented stable mechanical stability and durability. Lee et al. (91) fabricated

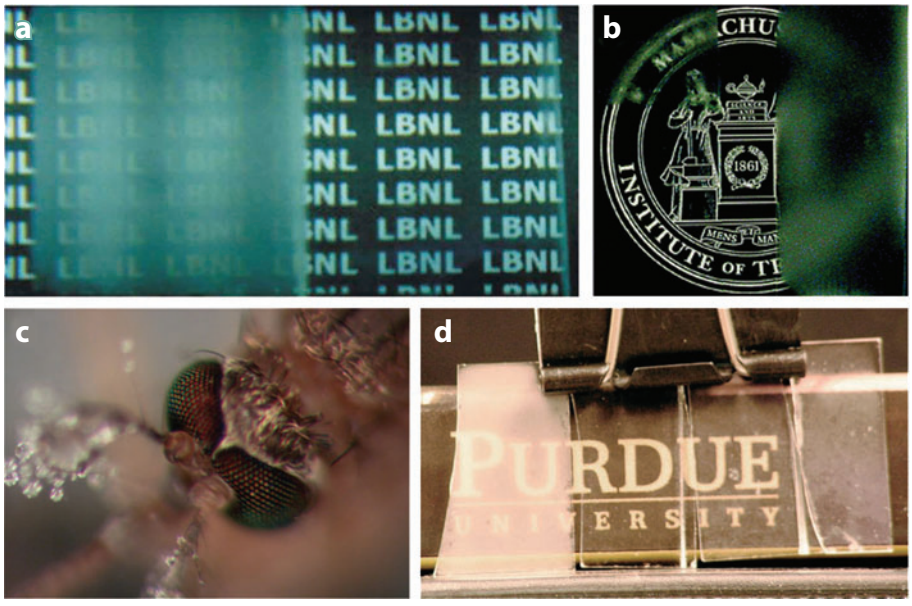

Figure 12

(*a*) Comparison of the antifogging property of a glass slide (*left*) and a self-similar porous TiO_2-coated glass slide (*right*) (89). (*b*) Image demonstrating the antifogging properties of multilayer coated glass (*left*) compared with that of an untreated glass substrate (*right*). Each sample was exposed to air (relative humidity approximately 50%) after being cooled in a refrigerator (below −4°C) for 12 h. The top portion of the slide on the left has not been coated with the multilayer; thus, it fogs and scatters light (91). (*c*) A photograph of antifogging mosquito compound eyes. Even exposed to moisture, mosquito eyes remain dry and clear while surrounding hairs nucleate many drops (93). (*d*) Fogging of various surfaces in response to being held over boiling water. From left to right: hydrophobized glass, two optimized f-PEG surfaces, and clean glass. Treated surfaces maintain less fogging than hydrophobized glass, which strongly fogs, or clean glass, which mildly fogs, due to adventitious oils (94).

multifunctional TiO_2/SiO_2 thin-film coatings with antifogging, superhydrophilicity, antireflection, and self-cleaning properties via a layer-by-layer deposition (**Figure 12*b***) arising from the presence of nanopores in the TiO_2/SiO_2 nanoparticle coatings. The superhydrophilicity of contaminated coatings could be readily recovered and retained after UV irradiation. Recently, Kwak et al. (92) prepared multifunctional transparent ZnO nanorod films using an ammonia hydrothermal method. In addition to antifogging, the obtained films demonstrated other properties, such as superhydrophilicity, high transmittance, UV protection, and antireflection.

Superhydrophobicity-induced antifogging. Mosquitoes possess excellent vision and can fly freely even in a watery and gloomy environment. Besides superhydrophobic self-cleaning, mosquito compound eyes exhibit antifogging and antireflection functionalities arising from their surface multiscale structures, which consist of hexagonally close-packed micro-ommatidia covered by hexagonally non-close-packed nanonipples (93). Tiny fog drops cannot stay on mosquito compound eye surfaces, thus inducing a dry, clear state even in foggy and moist environments (**Figure 12*c***). Inspired by mosquito compound eyes, multifunctional artificial compound eyes with superhydrophobicity and antifogging have been prepared using a soft lithography method followed by fluoroalkylsilane modification (93).

Stimuli-responsive polymer-induced antifogging. Oils fouling the surface were more difficult to remove due to their low surface energy. The contamination layer created a new surface and subsequently induced fogging rather than preventing it. Therefore, to obtain simultaneous self-cleaning and antifogging materials, it is essential to construct a novel functional surface possessing both hydrophilicity, necessary for antifogging, and oleophobicity, necessary for contamination resistance (95). Recently, a novel antifogging strategy was proposed by Howarter et al. (94) via stimuli-responsive polymer brushes. Perfluorinated end-capped polyethylene glycol (f-PEG) surfaces were fabricated through a grafting-to method. The resultant f-PEG surfaces exhibited stimuli-responsive and simultaneously PEG-like behavior to water (hydrophilicity) and fluorinated behavior to oil (oleophobicity), which is a promising solution for self-cleaning antifog coatings (**Figure 12*d***).

Anti-Icing

Ice formation has catastrophic consequences for human activity on the ground and in the air. Most current deicing approaches including physical or chemical removal of ice resulted in energy and resource costs as well as a negative impact on the environment. Therefore, rationally integrating anti-icing technology into material design is more efficient and sustainable than conventional solutions such as chemical sprays, salt, and heating. Recently, scientists and engineers have begun exploring the utility of superhydrophobic surfaces in delaying and reducing the accumulation of wet snow, ice, or frost (96–98).

Meuler et al. (99) investigated the relationships between water wettability and ice adhesion strength on nominally smooth bare and polymer-coated steel discs. It was found that maximizing the receding water contact angle could minimize ice adhesion. Tourkine et al. (100) demonstrated that freezing is significantly delayed when water is deposited on cold superhydrophobic copper surfaces. When the superhydrophobic copper plate is slightly tilted, water drops can be removed without freezing and accumulating on the substrate. Cao et al. (101) proved the superhydrophobic approach is a versatile strategy to avoid formation of ice. They studied icing of supercooled water on superhydrophobic surfaces fabricated using nanoparticle-polymer composites and found superhydrophobic surfaces could prevent ice formation upon impact of supercooled water both in laboratory conditions and in naturally occurring environments. The anti-icing property of these composites is dependent not only on their superhydrophobicity but also on the size of the particles exposed on the surface. Therefore, surface textures in multiple length scales should be considered during the construction of anti-icing superhydrophobic surfaces.

Recently, Mishchenko et al. (102) demonstrated a comprehensive experimental and theoretical study of dynamic droplet freezing on structured surfaces, where the properties and geometry of superhydrophobic surfaces, surface-liquid interactions, droplet dynamics, ice nucleation, and ice prevention were first integrated into one unified picture (**Figure 13**). The changes of wetting behavior on hydrophilic, hydrophobic, and superhydrophobic surfaces were also investigated. Research indicated that highly ordered micro/nanostructured superhydrophobic surfaces could be designed to remain entirely ice-free down to approximately −25 to −30°C owing to their ability to repel impacting water before ice nucleation occurs. This research provided an avenue for the rational design of anti-icing materials using multiscale structured superhydrophobic surfaces.

Icing of water on superhydrophobic surfaces is a complex phenomenon. Although a series of anti-icing materials have been fabricated, to design effective anti-icing materials through the superhydrophobic approach, further fundamental investigations are still necessary to study the effect of wettability, roughness, structure, and morphology on anti-icing performance (98, 103, 104). Deeper understanding of these features is essential for a rational design, the development

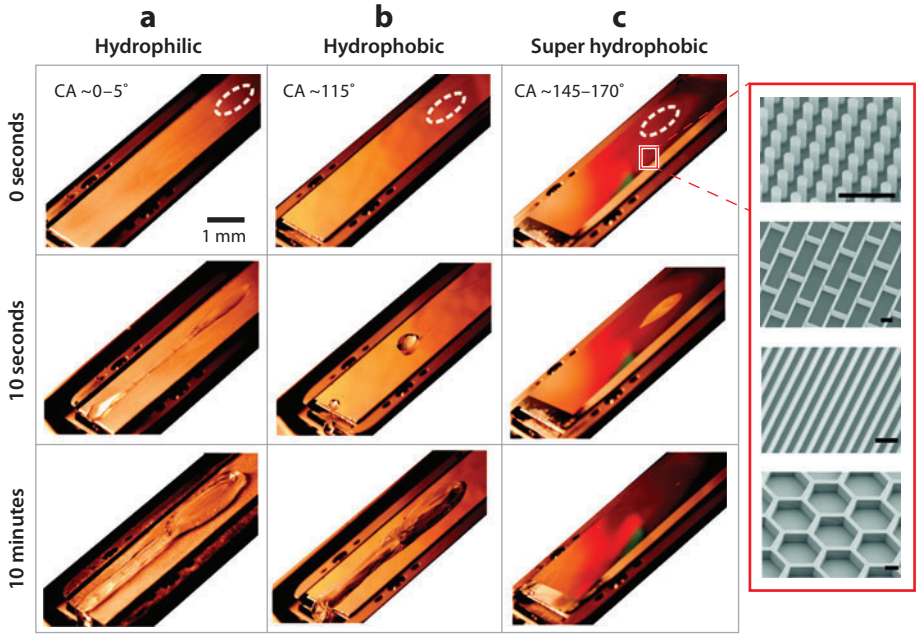

Figure 13

Ice accumulation on (*a*) flat aluminum, (*b*) smooth fluorinated Si, and (*c*) microstructured fluorinated Si surfaces. The advancing contact angle of the water droplets on these surfaces is indicated. Insets show micrographs of superhydrophobic surfaces: posts, bricks, blades, and honeycombs (scale bars: 10 μm). A stream of droplets ($T_{droplet} = 0°C$) was impinged from a 10 cm height at a rate of 0.06 ml s^{-1} onto surfaces ($T_{substrate} = -10°C$) tilted at 30°. White dashed circles indicate the position of droplet impact. Ice accumulation was observed on both hydrophilic and hydrophobic surfaces, whereas no freezing or accumulation was observed on the superhydrophobic surface even after a significant period of time (102).

of new synthesis routes, and the reproducible construction of anti-icing materials for practical applications.

Antireflection

TiO_2-based antireflection. TiO_2-based coatings can be applied easily on transparent substrates such as glass and plastic to obtain a self-cleaning property. However, these coatings always result in the surface reflection enhancement of transparent substrates owing to the large refractive index *n* of TiO_2 (approximately 2.52 for anatase and 2.76 for rutile). A general strategy for the construction of self-cleaning antireflective coatings is the combination of SiO_2 and TiO_2. An SiO_2 layer was used to provide a porous structure with low refractive index, which induced the antireflection effect, whereas TiO_2 nanoparticles coated on SiO_2 surfaces provided a superhydrophilic self-cleaning property. Recently, through the use of dip-coating, layer-by-layer assembly, sol-gel, or other approaches, a variety of coatings with self-cleaning and antireflection have been fabricated on different substrates (105–107). For example, superhydrophilic TiO_2/SiO_2 films with self-cleaning and antireflection were prepared through a layer-by-layer assembly process (107). The resultant coatings assembled with 10 cycles can reach effective photocatalysis with a maximum transmittance of 99.3% as well as a water droplet spreading time as short as 0.29 s.

Superhydrophobic antireflection. Superhydrophobic self-cleaning surfaces with high reflectivity have a wide variety of optical applications, ranging from traffic to solar energy industries. Using different synthesis strategies, researchers have constructed a wide variety of superhydrophobic materials with antireflection strategies (108–110). Subwavelength Si nanowire arrays with superhydrophobicity, self-cleaning, and antireflection were fabricated by Dai et al. (111) using a galvanic wet etching method. Fresnel reflection and diffuse reflection significantly over the broadband regions can be eliminated. The obtained subwavelength structures presented polarization-independent and omnidirectional antireflection properties. The diffuse reflectance and wavelength-averaged specular can reach as low as 2.51% and 0.06%, respectively.

Recently, Nakata et al. (112) fabricated self-cleaning antireflective surfaces using a moth-eye-like poly(ethylene terephthalate) film coated with TiO_2 particles. The obtained film exhibited a high transmittance of 76–95% and almost no absorption in the range of 400–800 nm. After irradiation with UV light, these films showed stable superhydrophilicity (at least 18 days). Antireflection is not restricted to the insect compound eyes; it has also been found on insect wings for the purpose of camouflage. For example, cicada wings possess not only superhydrophobic self-cleaning but antireflection functions. Inspired by both unique functionalities of cicada wings and moth eyes, Min et al. (113) developed a bio-inspired templating technique to fabricate multifunctional optical coatings.

Corrosion Resistance

Recently, superhydrophobic surfaces with anticorrosion properties have received much attention owing to their important industrial applications (114, 115). Grignard et al. (116) prepared stable superhydrophobic aluminum surfaces with excellent corrosion resistance by electrospinning of fluorinated diblock copolymer. The superhydrophobic effect resulted in the improvement of the corrosion inhibition. Lotus-inspired superhydrophobic Mg-Li alloy surfaces were fabricated by Liu et al. (117) using solution immersion and postmodification with fluoroalkylsilane. These resultant alloy surfaces possessing peony-like multiscale structures presented improved corrosion resistance and long-term stable superhydrophobicity with a small sliding angle. Ishizaki et al. (118) investigated the corrosion resistance and durability of superhydrophobic magnesium alloy coated with nanostructured cerium oxide film and fluoroalkylsilane molecules in the corrosive NaCl aqueous solution. The corrosion-resistant performance of the magnesium alloy was considerably improved due to the combination of superhydrophobic protective layers and the formation of $Mg(OH)_2$.

Drag Reduction

Drag is a major hindrance to movement. Inspired by natural materials with special drag reduction, different synthesis strategies have been developed to fabricate self-cleaning antidrag surfaces. Generally, drag-reducing surfaces can be achieved through the following two approaches: (*a*) shark skin–inspired surfaces for drag reduction and (*b*) superhydrophobic surfaces for drag reduction.

Shark skin–inspired drag reduction. Most shark species move in water with high efficiency and maintain buoyancy. In addition to the above-mentioned antifouling self-cleaning, shark skin also demonstrates surprisingly high drag reduction due to the ingenious antidrag design on the skin surfaces (80). Research indicates that shark skins possess small individual tooth-like scales (dermal denticles), which are ribbed with longitudinal grooves (aligned parallel to the local flow direction of the water). This special structure reduces the formation of vortices and results in water moving

efficiently over shark skin surfaces and drag reduction. Inspired by shark skin, a transparent plastic film with this same microscopic texture (79), ribs parallel to the direction of flow, was used on commercial aircraft, reducing aircraft drag by up to 8% with a fuel saving of approximately 1.5%. Inspired by the riblet effect of the shark skin, a variety of commercial swimsuits using new fibers and weaving techniques have been produced and used in swimming competitions, especially in the Olympic Games.

Superhydrophobicity-induced drag reduction. The other approach for the attainment of drag reduction is based on superhydrophobic surfaces (119, 120). The fluidic drag reduction of the superhydrophobic surface can be attributed to the superior water repellency of the surface, which dramatically reduces the interaction on the solid/water interface and generates a thin layer of air to establish a shear-free air/water interface over which water slips (121). Shi et al. (122) fabricated superhydrophobic gold threads and confirmed that superhydrophobic coatings can effectively reduce the fluidic drag for objects moving in water. With the same propulsion, the velocity of superhydrophobic gold threads is as much as 1.7 times that of normal hydrophobic gold threads. Su et al. (123) investigated the movement of superhydrophobic glass balls compared with hydrophilic balls. Faster movement of a superhydrophobic ball on the water surface can be observed, resulting from the increased area of the solid/air interface and the great reduction of skin friction. Under water, the superhydrophobic ball moved more slowly compared with the hydrophilic one owing to the dense microbubbles trapped at the solid/water interface around the superhydrophobic ball, resulting in the increase of friction drag. Recently, to construct mechanically durable structured surfaces with superhydrophobicity, self-cleaning, and low-drag properties, carbon nanotube composites were produced by replication of a micropatterned silicon surface by using an epoxy resin and deposition of the carbon nanotube composite (124). Superhydrophobic carbon nanotube composites with a low contact angle hysteresis exhibited stabile wetting properties and high mechanical strength and wear resistance. Although recent experimental and computational work demonstrated the superhydrophobic approach is a versatile and effective strategy for fluidic drag reduction, the construction of superhydrophobic drag reduction materials with improved stability used in the complicated real water environment is still a challenge.

Exterior Construction Materials

Research indicated the self-cleaning effect of TiO_2 surfaces can be enhanced when water flow, such as natural rainfall, was applied to the surface (21). Therefore, the best use of self-cleaning TiO_2 surfaces should be exterior construction materials because these materials could be exposed to abundant sunlight and natural rainfall. Since the late 1990s, a great number of hydrophilic self-cleaning coatings—including iles, glass, aluminum siding, plastic films, tent materials, cement, and others—have been commercialized (8, 9, 125). For example, in China, the National Opera Hall is covered by self-cleaning glass coated with a film of TiO_2 photocatalytic nanoparticles (**Figure 14*a***) (126). A white cement containing TiO_2 has been used for the construction of the *Dives in Misericordia* Church in Rome (**Figure 14*b***) (125). In Japan, several thousand tall buildings have been covered with self-cleaning tiles. Since 2003, the PanaHome Company, one of the major house manufacturers in Japan, has marketed "eco-life"-type houses, which utilize self-cleaning tiles and windows as well as a solar cell–covered rooftop (**Figure 14*c***) (9). The generalized use of self-cleaning surfaces will allow buildings to maintain their aesthetic appearance unaltered over time, which is very important in urban environments. Furthermore, self-cleaning technology results in large decreases in maintenance costs.

Figure 14

Applications of self-cleaning exterior building materials. (*a*) China's new National Opera Hall features self-cleaning glass coated with a film of photocatalytic nanoparticles that can break down dirt (126). (*b*) Rome's *Dives in Misericordia*, a church constructed of TiO_2-containing self-cleaning cement (125). (*c*) Japan's eco-life-type houses using self-cleaning tiles and glass (9).

Recently, Lee et al. (127) demonstrated elastomeric smart windows with self-cleaning and antireflection as well as mechanically tunable optical transparency and wetting properties. These stretchable smart windows were fabricated using wrinkled PDMS films through the combination of replica molding with nanoporous anodic aluminum oxide and surface wrinkling. The remarkable smart change can be attributed to the light-scattering properties and the discontinuous three-phase (solid-liquid-gas) contact line produced by microwrinkles tuned by applied mechanical strain.

Sensor

Clogging of membranes is a serious problem occurring in virtually all size separation devices with pore openings within the size range of the smallest excluded proteins. Recently, Roy et al. (128) prepared free-standing, self-cleaning nanochannel TiO_2 membranes for size-selective protein separation using a self-organizing process. Nanochannel TiO_2 membrane structures with both sides open can be formed in a single anodization step of a Ti-foil, where anatase crystallites can be directly formed. Therefore, when the membranes clog, they can easily be fully reopened and thus are reusable owing to the self-cleaning property of TiO_2. High-aspect-ratio self-organized TiO_2-nanotube layers were fabricated by Song et al. (129) through anodization of Ti-foils. These TiO_2-nanotube layers can be used as a self-cleaning platform for high-sensitivity immunoassays. Due to the photocatalytic self-cleaning property of TiO_2, the highly sensitive fluorescence sensor was reusable after a short UV treatment. Joo et al. (130) demonstrated ZnO nanorod-coated quartz crystals as thiol vapor sensors for natural gas fuel cells. Owing to the photocatalytic properties of ZnO, when thiol-adsorbed crystals were exposed to UV light, the adsorbed thiol molecules could be completely removed, demonstrating self-cleaning properties.

Carbon nanoparticles have drawn increasing attention due to their promising applications in bioimaging and optoelectronic devices. Recently, a highly flexible and sensitive infrared nanosensor with superhydrophobicity and self-cleaning was fabricated by Yuan et al. (131) using carbon nanoparticles through a flame method (**Figure 15**). The infrared nanosensor was constructed by transferring carbon nanoparticles to an optical transparent and flexible PDMS layer, demonstrating a sharp photoresponse with a response time of approximately 68 ms and a maximum photocurrent change of approximately 52.9%. The enhanced infrared photoresponse can be attributed to the photoinduced generation of excitons and thermal effects.

Cross-linked thermoresponsive hydrogels reversibly switch between a hydrophilic, swollen state and a hydrophobic, deswollen state through the adjustment of the volume phase transition temperature (VPTT). Thermoresponsive PNIPAAm hydrogels can be used to release cell sheets

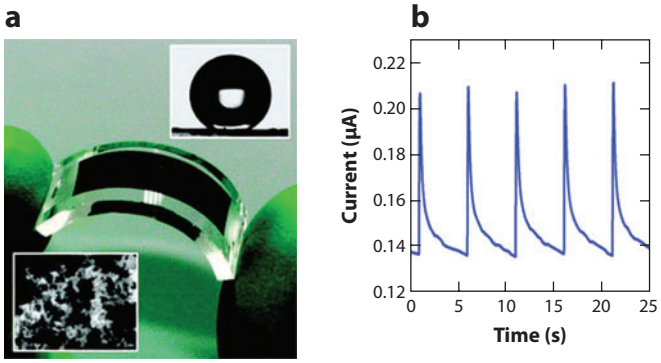

Figure 15

(*a*) Self-cleaning flexible infrared nanosensor based on carbon nanoparticles. Insets are an SEM image of carbon nanoparticles grown on ceramic strips and water drop profile on the superhydrophobic device surface. (*b*) Current change under the on/off incident pulsed infrared light (power density: 7.8 mW mm^{-2}; pulse width: 2 ms; period time: 5 s) (131).

from culture dishes without the use of potentially damaging enzymes or chelating agents. Gant et al. (132) developed a self-cleaning thermoresponsive nanocomposite hydrogel membrane for implantable optical glucose biosensors to control the host response. The introduction of hydrophilic *N*-vinylpyrrolidone results in the increase of VPTT above body temperature, good mechanical strength, glucose diffusion, and in vitro cell release upon thermal cycling. The thermal cycling schedule of the hydrogel was effective at limiting cell adhesion, demonstrating a self-cleaning property that could be used in vivo to minimize membrane biofouling of implanted sensors. When PNIPAAm polymers infiltrate vertically aligned carbon nanotubes, smart nanocomposite films with temperature-induced self-cleaning and controlled release capabilities are obtained through the synergetic effects (133). The self-cleaning and controlled release actions can be attributed to the temperature-induced reversible rod–coil conformational transition of PNIPAAm in an aqueous solution that results in the infiltrated polymer chains expanding out or collapsing within the nanotube gaps. Similar mechanism can also be found in self-cleaning resins (134), where organic solutes with different polarity can be adsorbed onto such resins while in the liquid-crystalline phase and released when converted into the gel phase.

Solar Cells

Recent research demonstrated that superhydrophobic self-cleaning surfaces can also be used in the solar cell field. Choi et al. (135) demonstrated biomimetic multiscale structures with transparent, antireflective, and superhydrophobic self-cleaning properties for organic solar cells. The multifunctional surface resulted in an enhancement of photovoltaic power conversion efficiency due to the reflection suppression and transmittance enhancement. Park et al. (136) fabricated superhydrophobic microshell structures with self-cleaning properties. Ordered microshell arrays were fabricated on a transparent and flexible PDMS elastomer surface. The microshell PDMS exhibited excellent superhydrophobic and water-repellent properties without chemical modification. The degradation of solar cell efficiency by airborne dust can be reduced by covering the solar cell module with self-cleaning PDMS arrays. Zhu et al. (137) fabricated nanodome solar cell devices with effective antireflection and light trapping over a broad spectral range. After

modification with hydrophobic molecules, nanodome solar cells presented superhydrophobic self-cleaning properties. The power efficiency of nanodome solar cells is higher than that of flat-film devices.

Textiles

Self-cleaning technology has been successfully used in the field of textiles. In this section, we mainly discuss self-cleaning textiles through the pure-TiO_2, TiO_2-based composites, and superhydrophobic approaches.

Self-cleaning textiles using pure TiO_2. TiO_2-coated textiles are another important application of self-cleaning technology (138). Abidi et al. (139) investigated the self-cleaning performance of cotton fabric surfaces modified with TiO_2 nanosols via the sol-gel approach. It was found that coffee and red wine stains on TiO_2-nanosol-treated cotton can be decomposed under UV radiation. Furthermore, TiO_2-nanosol treatment imparted excellent UV-radiation protection to the cotton fabric. Coaxial electrospinning proved to be versatile for the fabrication of photocatalytic self-cleaning textile nanofibers with high surface-to-volume ratio. When cellulose acetate and TiO_2 were used as the core phase and sheath phase, respectively (140), the obtained photocatalytic fibers could maintain their self-cleaning properties after multiple staining and washing steps.

Self-cleaning textiles using TiO_2-based composites. Due to wide band gaps, TiO_2 photocatalysts mainly absorb UV photons. However, solar light contains only a small amount of UV photons (approximately 5%). Therefore, to extend the spectral response of TiO_2 from UV light to visible light, a variety of synthesis strategies have been proposed (9). For example, to reduce the negative effect of TiO_2 and improve the visible-light self-cleaning performance, porous $Au/TiO_2/SiO_2$ nanocomposites were fabricated by Wang et al. (141) using sol-gel nanotechnology. $Au/TiO_2/SiO_2$-coated cotton fabrics did not change their appearance color. Red wine stains and coffee stains applied to the fabric could be self-cleaned after visible-light irradiation for 20 h. The presence of Au species may improve the rate of electron transfer to oxygen and then decrease the rate of recombination between excited electron/hole pairs. Usually, the presence of silica could increase the photocatalytic activity of TiO_2, arising from the high dispersion and the structural effects of the amorphous silica. Yuranova et al. (142) demonstrated transparent photoactive coatings of TiO_2-SiO_2 with self-cleaning properties through a sol-gel method. The resultant TiO_2-SiO_2 coatings exhibited superior photocatalytic and self-cleaning properties in comparison with pure TiO_2.

Self-cleaning textiles via a superhydrophobic approach. As mentioned above, superhydrophobic surfaces with a low sliding angle demonstrated a self-cleaning property (lotus effect), which can be used in self-cleaning textiles. Contaminants, either inorganic or organic, adhere to water droplets and are removed from the surface when the water rolls off.

Mimicking the self-cleaning and miniature protrusions of the lotus leaves, Ramaratnam et al. (143) prepared superhydrophobic self-cleaning textiles by decorating fibers with reactive SiO_2 nanoparticle monolayers and nonfluorinated polymers. Water droplets rolled over the textile material, collected the dirt, and then cleaned the fabric, which is similar to the lotus effect. The hybrid coating can be permanently anchored to the fiber boundary due to the chemical attachment of the nanoparticles and polymers to the surface. Nano-Tex has a range of superhydrophobic self-cleaning products to resist spills, repel and release stains, and resist static. The author's group developed a two-step procedure to obtain self-cleaning superamphiphobic textiles by low-temperature

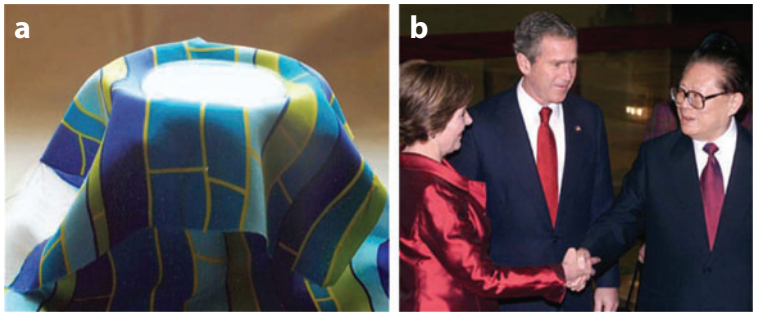

Figure 16

(*a*) The product of superamphiphobic textiles with self-cleaning properties (13). (*b*) The self-cleaning nanotie presented to former US President George Bush and former Chinese President Jiang Zemin in 2002 (144).

plasma treatment followed by modification with fluorocarbons (144). The self-cleaning nanotie can repel both water-based and oil-based liquids (**Figure 16**).

Others

In addition to the above-described applications, self-cleaning surfaces also demonstrate important applications in antibacterial, structural color, flame retardant, shielding, water treatment, and other fields (145, 146). Sulfur-doped TiO_2 films with self-cleaning were fabricated by Dunnill et al. (147) using atmospheric pressure chemical vapor deposition. The incorporation of sulfur into TiO_2 enhanced the photocatalytic properties and photo-induced superhydrophilicity, which can kill the bacterium *Escherichia coli* using white light. Cao et al. (148) prepared flowerlike $Mg(OH)_2$ complex nanostructures with superhydrophobicity and self-cleaning and flame retardant effects using an amino acid–assisted hydrothermal approach. Bormashenko et al. (149) demonstrated that superhydrophobic surfaces could be exploited for smart manipulation of droplets, i.e., cutting of droplets with two-sided superhydrophobic blade (**Figure 17**). Nonstick droplets could also be cut with a superhydrophobic scalpel, exhibiting the potential for microfluidics and biomedical applications. Polymer-based large-area superhydrophobic self-cleaning carbon nanofiber composite coatings were prepared for tunable electromagnetic interference shielding and attenuation in the terahertz frequency regime (150). Recently, a novel electrocatalytic membrane reactor with self-cleaning function was fabricated for industrial wastewater treatment (151), which demonstrated superior performance in the treatment of oily water compared with conventional membrane filtration.

Figure 17

Cutting Janus marbles. (*a*) An initial 200 μl Janus marble coated partially with carbon black and partially with Teflon. (*b*) Cutting the Janus marble. (*c*) Separated marbles (149).

REMAINING CHALLENGES AND FUTURE OUTLOOK

In this review, the recent developments in the mechanism, fabrication, and application of self-cleaning surfaces—including TiO_2-based, lotus effect–inspired, gecko setae–inspired, and underwater organisms–inspired self-cleaning surfaces—are described. In the past few decades, a great number of self-cleaning surfaces have been constructed and commercialized utilizing different synthesis strategies. However, to stimulate and extend the applications of self-cleaning surfaces, further research is of great importance for fundamental research and practical applications, which has become an increasingly hot research topic. In the near future, the following research directions should be addressed.

For TiO_2-based self-cleaning surfaces, although a great variety of commercial self-cleaning products have become available to the consumer, a deeper understanding of the mechanism is still needed. Further fundamental investigations of TiO_2-based self-cleaning mechanisms would be helpful to further extend the absorption range into the visible region, improve self-cleaning efficiency, and then expand the application field of self-cleaning surfaces. During the practical application of self-cleaning surfaces, sufficient mechanical and thermal stability should also be considered.

Creating multifunctional materials is an eternal goal for human beings. The fusion of two or more functions into a unique composite is an exciting direction for the fabrication of novel multifunctional self-cleaning surfaces. For example, Faustini et al. (152) recently demonstrated that self-cleaning, antireflection, water repellence, antifogging, and relatively high mechanical properties can be integrated into a sol-gel coating composed of a methyl-modified SiO_2 and TiO_2 bilayer. These multifunctional nanostructured materials deposited onto glass substrates can be used for photovoltaic cells.

Design and construction of smart self-cleaning surfaces with self-healing will be another research focus in the future. Learning from nature has long been a source of bioinspiration for scientists and engineers (153). For example, inspired by *Nepenthes* pitcher plants, Wong et al. (154) recently fabricated self-healing, slippery liquid–infused porous surfaces with enhanced optical transparency. Furthermore, these smart porous surfaces outperform their natural counterparts and can repel various liquids (water, hydrocarbons, crude oil, and blood) and even insects, maintain low contact angle hysteresis, quickly restore liquid repellency after physical damage, resist ice adhesion, and function at high pressures. The obtained multifunctional smart surfaces will be useful in fluid handling and transportation, optical sensing, and medicine and as self-cleaning and antifouling materials operating in extreme environments. Nature has evolved different solutions to achieve efficient multifunctional integration. Optimized biological solutions continue to inspire and to provide design principles for the rational design and construction of multifunctional smart surfaces. Therefore, further interdisciplinary cooperation is necessary to design multifunctional smart self-cleaning surfaces for researchers in the area of science and engineering.

DISCLOSURE STATEMENT

The authors are not aware of any affiliations, memberships, funding, or financial holdings that might be perceived as affecting the objectivity of this review.

ACKNOWLEDGMENTS

We appreciate the financial support of the National Natural Science Foundation of China (21001013), the National Basic Research Program of China (2010CB934700), the Program for

New Century Excellent Talents in University, the Beijing Natural Science Foundation (2122035), the Specialized Research Fund for the Doctoral Program of Higher Education, and the Fundamental Research Funds for the Central Universities.

LITERATURE CITED

1. Quéré D. 2008. Wetting and roughness. *Annu. Rev. Mater. Res.* 38:71–99
2. Liu KS, Yao X, Jiang L. 2010. Recent developments in bio-inspired special wettability. *Chem. Soc. Rev.* 39:3240–55
3. Bhushan B, Jung YC. 2011. Natural and biomimetic artificial surfaces for superhydrophobicity, self-cleaning, low adhesion, and drag reduction. *Prog. Mater. Sci.* 56:1–108
4. Genzer J, Marmur A. 2008. Biological and synthetic self-cleaning surfaces. *MRS Bull.* 33:742–46
5. Genzer J, Efimenko K. 2006. Recent developments in superhydrophobic surfaces and their relevance to marine fouling: a review. *Biofouling* 22:339–60
6. Zhang X, Shi F, Niu J, Jiang YG, Wang ZQ. 2008. Superhydrophobic surfaces: from structural control to functional application. *J. Mater. Chem.* 18:621–33
7. Blossey R. 2003. Self-cleaning surfaces—virtual realities. *Nat. Mater.* 2:301–6
8. Parkin IP, Palgrave RG. 2005. Self-cleaning coatings. *J. Mater. Chem.* 15:1689–95
9. Fujishima A, Zhang XT, Tryk DA. 2008. TiO_2 photocatalysis and related surface phenomena. *Surf. Sci. Rep.* 63:515–82
10. Quéré D, Reyssat M. 2008. Non-adhesive lotus and other hydrophobic materials. *Philos. Trans. R. Soc. A* 366:1539–56
11. Liu KS, Jiang L. 2011. Bio-inspired design of multiscale structures for function integration. *Nano Today* 6:155–75
12. Ganesh VA, Raut HK, Nair AS, Ramakrishna S. 2011. A review on self-cleaning coatings. *J. Mater. Chem.* 21:16304–2211
13. Yao X, Song YL, Jiang L. 2011. Applications of bio-inspired special wettable surfaces. *Adv. Mater.* 23:719–34
14. Young T. 1805. An essay on the cohesion of fluids. *Philos. Trans. R. Soc. Lond.* 95:65–87
15. Wenzel RN. 1936. Resistance of solid surfaces to wetting by water. *Ind. Eng. Chem.* 28:988–94
16. Cassie ABD, Baxter S. 1944. Wettability of porous surfaces. *Trans. Faraday Soc.* 40:546–51
17. Lafuma A, Quéré D. 2003. Superhydrophobic states. *Nat. Mater.* 2:457–60
18. Koishi T, Yasuoka K, Fujikawa S, Ebisuzaki T, Zeng XC. 2009. Coexistence and transition between Cassie and Wenzel state on pillared hydrophobic surface. *Proc. Natl. Acad. Sci. USA* 106:8435–40
19. Forsberg P, Nikolajeff F, Karlsson M. 2011. Cassie-Wenzel and Wenzel-Cassie transitions on immersed superhydrophobic surfaces under hydrostatic pressure. *Soft Matter* 7:104–9
20. Wang R, Hashimoto K, Fujishima A, Chikuni M, Kojima E, et al. 1997. Light-induced amphiphilic surfaces. *Nature* 388:431–32
21. Wang R, Hashimoto K, Fujishima A, Chikuni M, Kojima E, et al. 1998. Photogeneration of highly amphiphilic TiO_2 surfaces. *Adv. Mater.* 10:135–38
22. Neinhuis C, Barthlott W. 1997. Characterization and distribution of water-repellent, self-cleaning plant surfaces. *Ann. Bot.* 79:667–77
23. Feng L, Li SH, Li YS, Li HJ, Zhang LJ, et al. 2002. Super-hydrophobic surfaces: from natural to artificial. *Adv. Mater.* 14:1857–60
24. Watson GS, Cribb BW, Watson JA. 2010. How micro/nanoarchitecture facilitates anti-wetting: an elegant hierarchical design on the termite wing. *ACS Nano* 4:129–36
25. Liu KS, Fu HG, Shi KH, Xin BF, Jing LQ, Zhou W. 2006. Hydrophilicity and formation mechanism of large-pore mesoporous TiO_2 thin films with tunable pore diameters. *Nanotechnology* 17:3641–48
26. Xu QC, Wellia DV, Sk MA, Lim KH, Loo JSC, et al. 2010. Transparent visible light activated C-N-F-codoped TiO_2 films for self-cleaning applications. *J. Photochem. Photobiol. A* 210:181–87
27. Liu KS, Zhang ML, Zhou W, Li L, Wang J, Fu HG. 2005. Preparation, characterization, and photo-induced hydrophilicity of nanocrystalline anatase thin films synthesized through evaporation-induced assembly. *Nanotechnology* 16:3006–11

28. Liu KS, Zhou W, Shi KY, Li L, Zhang LL, et al. 2006. Influence of calcination temperatures on the photocatalytic activity and photo-induced hydrophilicity of wormhole-like mesoporous TiO_2. *Nanotechnology* 17:1363–69
29. Li Y, Sasaki T, Shimizu Y, Koshizaki N. 2008. Hexagonal-close-packed, hierarchical amorphous TiO_2 nanocolumn arrays: transferability, enhanced photocatalytic activity, and superamphiphilicity without UV irradiation. *J. Am. Chem. Soc.* 130:14755–62
30. Daoud WA, Leung SK, Tung WS, Xin JH, Cheuk K, Qi K. 2008. Self-cleaning keratins. *Chem. Mater.* 20:1242–44
31. Soler-illia GJD, Sanchez C, Lebeau B, Patarin J. 2002. Chemical strategies to design textured materials: from microporous and mesoporous oxides to nanonetworks and hierarchical structures. *Chem. Rev.* 102:4093–138
32. Liu KS, Fu HG, Shi KY, Xiao FS, Jing LQ, Xin BF. 2005. Preparation of large-pore mesoporous nanocrystalline TiO_2 thin films with tailored pore diameters. *J. Phys. Chem. B* 109:18719–22
33. Liu K, Zhang M, Shi K, Fu H. 2005. Large-pore mesoporous nanocrystalline titania thin films synthesized through evaporation-induced self-assembly. *Mater. Lett.* 59:3308–10
34. Zhou W, Liu KS, Fu HG, Pan K, Zhang LL, et al. 2008. Multi-modal mesoporous TiO_2-ZrO_2 composites with high photocatalytic activity and hydrophilicity. *Nanotechnology* 19:035610
35. Allain E, Besson S, Durand C, Moreau M, Gacoin T, Boilot JP. 2007. Transparent mesoporous nanocomposite films for self-cleaning applications. *Adv. Funct. Mater.* 17:549–54
36. Fateh R, Ismail AA, Dillert R, Bahnemann DW. 2011. Highly active crystalline mesoporous TiO_2 films coated onto polycarbonate substrates for self-cleaning applications. *J. Phys. Chem. C* 115:10405–11
37. Bhushan B, Jung YC, Koch K. 2009. Self-cleaning efficiency of artificial superhydrophobic surfaces. *Langmuir* 25:3240–48
38. Nyström D, Lindqvist J, Östmark E, Hult A, Malmström E. 2006. Superhydrophobic bio-fibre surfaces via tailored grafting architecture. *Chem. Commun.* 42:3594–96
39. Nyström D, Lindqvist J, Östmark E, Antoni P, Carlmark A, et al. 2009. Superhydrophobic and self-cleaning bio-fiber surfaces via ATRP and subsequent postfunctionalization. *ACS Appl. Mater. Interfaces* 1:816–23
40. Kim TI, Tahk D, Lee HH. 2009. Wettability-controllable super water- and moderately oil-repellent surface fabricated by wet chemical etching. *Langmuir* 25:6576–79
41. Zhao K, Liu KS, Li JF, Wang WH, Jiang L. 2009. Superamphiphobic CaLi-based bulk metallic glasses. *Scr. Mater.* 60:225–27
42. Qi DAP, Lu N, Xu HB, Yang BJ, Huang CY, et al. 2009. Simple approach to wafer-scale self-cleaning antireflective silicon surfaces. *Langmuir* 25:7769–72
43. Xiu YH, Liu Y, Hess DW, Wong CP. 2010. Mechanically robust superhydrophobicity on hierarchically structured Si surfaces. *Nanotechnology* 21:155705
44. Hozumi A, McCarthy TJ. 2010. Ultralyophobic oxidized aluminum surfaces exhibiting negligible contact angle hysteresis. *Langmuir* 26:2567–73
45. Jiang L, Zhao Y, Zhai J. 2004. A lotus-leaf-like superhydrophobic surface: a porous microsphere/nanofiber composite film prepared by electrohydrodynamics. *Angew. Chem. Int. Ed.* 43:4338–41
46. Asmatulu R, Ceylan M, Nuraje N. 2011. Study of superhydrophobic electrospun nanocomposite fibers for energy systems. *Langmuir* 27:504–7
47. Lin JY, Cai Y, Wang XF, Ding B, Yu JY, Wang MR. 2011. Fabrication of biomimetic superhydrophobic surfaces inspired by lotus leaf and silver ragwort leaf. *Nanoscale* 3:1258–62
48. Liu KS, Zhai J, Jiang L. 2008. Fabrication and characterization of superhydrophobic Sb_2O_3 films. *Nanotechnology* 19:165604
49. Guo Z, Chen X, Li J, Liu JH, Huang XJ. 2011. ZnO/CuO hetero-hierarchical nanotrees array: hydrothermal preparation and self-cleaning properties. *Langmuir* 27:6193–200
50. Wang CF, Chen WY, Cheng HZ, Fu SL. 2010. Pressure-proof superhydrophobic films from flexible carbon nanotube/polymer coatings. *J. Phys. Chem. C* 114:15607–11
51. Cho WK, Park S, Jon S, Choi IS. 2007. Water-repellent coating: formation of polymeric self-assembled monolayers on nanostructured surfaces. *Nanotechnology* 18:395602

52. Li LH, Chen Y. 2010. Superhydrophobic properties of nonaligned boron nitride nanotube films. *Langmuir* 26:5135–40
53. Pakdel A, Zhi CY, Bando Y, Nakayama T, Golberg D. 2011. Boron nitride nanosheet coatings with controllable water repellency. *ACS Nano* 5:6507–15
54. Hsieh CT, Chen WY. 2010. Water/oil repellency and drop sliding behavior on carbon nanotubes/carbon paper composite surfaces. *Carbon* 48:612–19
55. Zhang YY, Stan L, Xu P, Wang HL, Doorn SK, et al. 2009. A double-layered carbon nanotube array with super-hydrophobicity. *Carbon* 47:3332–36
56. Yang HT, Jiang P. 2010. Self-cleaning diffractive macroporous films by doctor blade coating. *Langmuir* 26:12598–604
57. Zou JH, Chen H, Chunder A, Yu YX, Huo Q, Zhai L. 2008. Preparation of a superhydrophobic and conductive nanocomposite coating from a carbon-nanotube-conjugated block copolymer dispersion. *Adv. Mater.* 20:3337–41
58. Han JT, Kim SY, Woo JS, Lee GW. 2008. Transparent, conductive, and superhydrophobic films from stabilized carbon nanotube/silane sol mixture solution. *Adv. Mater.* 20:3724–27
59. Im M, Im H, Lee JH, Yoon JB, Choi YK. 2010. A robust superhydrophobic and superoleophobic surface with inverse-trapezoidal microstructures on a large transparent flexible substrate. *Soft Matter* 6:1401–4
60. Lee JS, Ryu J, Park CB. 2009. Bio-inspired fabrication of superhydrophobic surfaces through peptide self-assembly. *Soft Matter* 5:2717–20
61. Lee EJ, Kim JJ, Cho SO. 2010. Fabrication of porous hierarchical polymer/ceramic composites by electron irradiation of organic/inorganic polymers: route to a highly durable, large-area superhydrophobic coating. *Langmuir* 26:3024–30
62. Ding XF, Zhou SX, Gu GX, Wu LM. 2011. A facile and large-area fabrication method of superhydrophobic self-cleaning fluorinated polysiloxane/TiO_2 nanocomposite coatings with long-term durability. *J. Mater. Chem.* 21:6161–64
63. Hwang HS, Kim NH, Lee SG, Lee DY, Cho K, Park I. 2011. Facile fabrication of transparent superhydrophobic surfaces by spray deposition. *ACS Appl. Mater. Interfaces* 3:2179–83
64. Niu JJ, Wang JN. 2009. A novel self-cleaning coating with silicon carbide nanowires. *J. Phys. Chem. B* 113:2909–12
65. Xu QF, Wang JN, Sanderson KD. 2010. A general approach for superhydrophobic coating with strong adhesion strength. *J. Mater. Chem.* 20:5961–66
66. Autumn K, Sitti M, Liang YCA, Peattie AM, Hansen WR, et al. 2002. Evidence for van der Waals adhesion in gecko setae. *Proc. Natl. Acad. Sci. USA* 99:12252–56
67. Liu K, Du J, Wu J, Jiang L. 2012. Superhydrophobic gecko feet with high adhesive forces towards water and their bio-inspired materials. *Nanoscale* 4:768–72
68. Autumn K, Gravish N. 2008. Gecko adhesion: evolutionary nanotechnology. *Philos. Trans. R. Soc. A* 366:1575–90
69. Hansen WR, Autumn K. 2005. Evidence for self-cleaning in gecko setae. *Proc. Natl. Acad. Sci. USA* 102:385–89
70. Lee J, Fearing RS. 2008. Contact self-cleaning of synthetic gecko adhesive from polymer microfibers. *Langmuir* 24:10587–91
71. Sethi S, Ge L, Ci L, Ajayan PM, Dhinojwala A. 2008. Gecko-inspired carbon nanotube-based self-cleaning adhesives. *Nano Lett.* 8:822–25
72. Kim S, Cheung E, Sitti M. 2009. Wet self-cleaning of biologically inspired elastomer mushroom shaped microfibrillar adhesives. *Langmuir* 25:7196–99
73. Davies J, Haq S, Hawke T, Sargent JP. 2009. A practical approach to the development of a synthetic gecko tape. *Int. J. Adhes. Adhes.* 29:380–90
74. Kustandi TS, Samper VD, Yi DK, Ng WS, Neuzil P, Sun WX. 2007. Self-assembled nanoparticles based fabrication of gecko foot-hair-inspired polymer nanofibers. *Adv. Funct. Mater.* 17:2211–18
75. Ko H, Zhang ZX, Chueh YL, Ho JC, Lee J, et al. 2009. Wet and dry adhesion properties of self-selective nanowire connectors. *Adv. Funct. Mater.* 19:3098–102

76. Magin CM, Cooper SP, Brennan AB. 2010. Non-toxic antifouling strategies. *Mater. Today* 13:36–44
77. Scardino AJ, de Nys R. 2011. Mini review: biomimetic models and bioinspired surfaces for fouling control. *Biofouling* 27:73–86
78. Bechert DW, Bruse M, Hage W. 2000. Experiments with three-dimensional riblets as an idealized model of shark skin. *Exp. Fluids* 28:403–12
79. Ball P. 1999. Shark skin and other solutions. *Nature* 400:507–9
80. Bhushan B. 2009. Biomimetics: lessons from nature—an overview. *Philos. Trans. R. Soc. A* 367:1445–86
81. Carman ML, Estes TG, Feinberg AW, Schumacher JF, Wilkerson W, et al. 2006. Engineered antifouling microtopographies—correlating wettability with cell attachment. *Biofouling* 22:11–21
82. Baum C, Meyer W, Stelzer R, Fleischer LG, Siebers D. 2002. Average nanorough skin surface of the pilot whale (*Globicephala melas*, Delphinidae): considerations on the self-cleaning abilities based on nanoroughness. *Mar. Biol.* 140:653–57
83. Baum C, Simon F, Meyer W, Fleischer LG, Siebers D, et al. 2003. Surface properties of the skin of the pilot whale *Globicephala melas*. *Biofouling* 19:181–86
84. Cao XY, Pettitt ME, Wode F, Sancet MPA, Fu JH, et al. 2010. Interaction of zoospores of the green alga *Ulva* with bioinspired micro- and nanostructured surfaces prepared by polyelectrolyte layer-by-layer self-assembly. *Adv. Funct. Mater.* 20:1984–93
85. Liu MJ, Wang ST, Wei ZX, Song YL, Jiang L. 2009. Bioinspired design of a superoleophobic and low adhesive water/solid interface. *Adv. Mater.* 21:665–69
86. Lin L, Liu MJ, Chen L, Chen PP, Ma J, et al. 2010. Bio-inspired hierarchical macromolecule-nanoclay hydrogels for robust underwater superoleophobicity. *Adv. Mater.* 22:4826–30
87. Pugno NM. 2007. Towards a Spiderman suit: large invisible cables and self-cleaning releasable superadhesive materials. *J. Phys.: Condens. Matter* 19:395001
88. Marmur A. 2006. Super-hydrophobicity fundamentals: implications to biofouling prevention. *Biofouling* 22:107–15
89. Zorba V, Chen XB, Mao SS. 2010. Superhydrophilic TiO_2 surface without photocatalytic activation. *Appl. Phys. Lett.* 96:093702
90. Li Y, Zhang J, Zhu S, Dong H, Jia F, et al. 2009. Biomimetic surfaces for high-performance optics. *Adv. Mater.* 21:4731–34
91. Lee D, Rubner MF, Cohen RE. 2006. All-nanoparticle thin-film coatings. *Nano Lett.* 6:2305–12
92. Kwak G, Jung S, Yong K. 2011. Multifunctional transparent ZnO nanorod films. *Nanotechnology* 22:115705
93. Gao XF, Yan X, Yao X, Xu L, Zhang K, et al. 2007. The dry-style antifogging properties of mosquito compound eyes and artificial analogues prepared by soft lithography. *Adv. Mater.* 19:2213–17
94. Howarter JA, Youngblood JP. 2007. Self-cleaning and anti-fog surfaces via stimuli-responsive polymer brushes. *Adv. Mater.* 19:3838–43
95. Howarter JA, Youngblood JP. 2008. Self-cleaning and next generation anti-fog surfaces and coatings. *Macromol. Rapid Commun.* 29:455–66
96. Sarkar DK, Farzaneh M. 2009. Superhydrophobic coatings with reduced ice adhesion. *J. Adhes. Sci. Technol.* 23:1215–37
97. Varanasi KK, Deng T, Smith JD, Hsu M, Bhate N. 2010. Frost formation and ice adhesion on superhydrophobic surfaces. *Appl. Phys. Lett.* 97:234102
98. Meuler AJ, McKinley GH, Cohen RE. 2010. Exploiting topographical texture to impart icephobicity. *ACS Nano* 4:7048–52
99. Meuler AJ, Smith JD, Varanasi KK, Mabry JM, McKiney GH, Cohen RE. 2010. Relationships between water wettability and ice adhesion. *ACS Appl. Mater. Interfaces* 2:3100–10
100. Tourkine P, Le Merrer M, Quéré D. 2009. Delayed freezing on water repellent materials. *Langmuir* 25:7214–16
101. Cao L, Jones AK, Sikka VK, Wu J, Gao D. 2009. Anti-icing superhydrophobic coatings. *Langmuir* 25:12444–48
102. Mishchenko L, Hatton B, Bahadur V, Taylor JA, Krupenkin T, Aizenberg J. 2010. Design of ice-free nanostructured surfaces based on repulsion of impacting water droplets. *ACS Nano* 4:7699–707

103. Kulinich SA, Farhadi S, Nose K, Du XW. 2011. Superhydrophobic surfaces: Are they really ice-repellent?*Langmuir* 27:25–29
104. Jung S, Dorrestijn M, Raps D, Das A, Megaridis CM, Poulikakos D. 2011. Are superhydrophobic surfaces best for icephobicity? *Langmuir* 27:3059–66
105. Liu ZY, Zhang XT, Murakami T, Fujishima A. 2008. Sol-gel SiO_2/TiO_2 bilayer films with self-cleaning and antireflection properties. *Sol. Energy Mater.* 92:1434–38
106. Prado R, Beobide G, Marcaide A, Goikoetxea J, Aranzabe A. 2010. Development of multifunctional sol-gel coatings: anti-reflection coatings with enhanced self-cleaning capacity. *Sol. Energy Mater.* 94:1081–88
107. Wang HT, Hu YJ, Zhang L, Li CZ. 2010. Self-cleaning films with high transparency based on TiO_2 nanoparticles synthesized via flame combustion. *Ind. Eng. Chem. Res.* 49:3654–62
108. Manca M, Cannavale A, De Marco L, Arico AS, Cingolani R, Gigli G. 2009. Durable superhydrophobic and antireflective surfaces by trimethylsilanized silica nanoparticles-based sol-gel processing. *Langmuir* 25:6357–62
109. Li XY, Du X, He JH. 2010. Self-cleaning antireflective coatings assembled from peculiar mesoporous silica nanoparticles. *Langmuir* 26:13528–34
110. Li YF, Zhang JH, Yang B. 2010. Antireflective surfaces based on biomimetic nanopillared arrays. *Nano Today* 5:117–27
111. Dai YA, Chang HC, Lai KY, Lin CA, Chung RJ, et al. 2010. Subwavelength Si nanowire arrays for self-cleaning antireflection coatings. *J. Mater. Chem.* 20:10924–30
112. Nakata KNK, Sakai M, Ochiai T, Murakami T, Takagi K, Fujishima A. 2011. Antireflection and self-cleaning properties of a moth-eye-like surface coated with TiO_2 particles. *Langmuir* 27:3275–78
113. Min WL, Jiang B, Jiang P. 2008. Bioinspired self-cleaning antireflection coatings. *Adv. Mater.* 20:3914–18
114. Liu K, Jiang L. 2011. Metallic surfaces with special wettability. *Nanoscale* 3:825–38
115. Liu K, Li Z, Wang W, Jiang L. 2011. Facile creation of bio-inspired superhydrophobic Ce-based metallic glass surfaces. *Appl. Phys. Lett.* 99:261905
116. Grignard B, Vaillant A, de Coninck J, Piens M, Jonas AM, et al. 2011. Electrospinning of a functional perfluorinated block copolymer as a powerful route for imparting superhydrophobicity and corrosion resistance to aluminum substrates. *Langmuir* 27:335–42
117. Liu KS, Zhang ML, Zhai J, Wang J, Jiang L. 2008. Bioinspired construction of Mg-Li alloys surfaces with stable superhydrophobicity and improved corrosion resistance. *Appl. Phys. Lett.* 92:183103
118. Ishizaki TIT, Masuda Y, Sakamoto M. 2011. Corrosion resistance and durability of superhydrophobic surface formed on magnesium alloy coated with nanostructured cerium oxide film and fluoroalkylsilane molecules in corrosive NaCl aqueous solution. *Langmuir* 27:4780–88
119. Rothstein JP. 2010. Slip on superhydrophobic surfaces. *Annu. Rev. Fluid Mech.* 42:89–109
120. McHale G, Newton MI, Shirtcliffe NJ. 2010. Immersed superhydrophobic surfaces: gas exchange, slip, and drag reduction properties. *Soft Matter* 6:714–19
121. Truesdell R, Mammoli A, Vorobieff P, van Swol F, Brinker CJ. 2006. Drag reduction on a patterned superhydrophobic surface. *Phys. Rev. Lett.* 97:044504
122. Shi F, Niu J, Liu JL, Liu F, Wang ZQ, et al. 2007. Towards understanding why a superhydrophobic coating is needed by water striders. *Adv. Mater.* 19:2257–61
123. Su B, Li M, Lu QH. 2010. Toward understanding whether superhydrophobic surfaces can really decrease fluidic friction drag. *Langmuir* 26:6048–52
124. Jung YC, Bhushan B. 2009. Mechanically durable carbon nanotube-composite hierarchical structures with superhydrophobicity, self-cleaning, and low-drag. *ACS Nano* 3:4155–63
125. Cassar L. 2004. Photocatalysis of cementitious materials: clean buildings and clean air. *MRS Bull.* 29:328–31
126. Bai C. 2005. Ascent of nanoscience in China. *Science* 309:61–63
127. Lee SG, Lee DY, Lim HS, Lee DH, Lee S, Cho K. 2010. Switchable transparency and wetting of elastomeric smart windows. *Adv. Mater.* 22:5013–17

128. Roy P, Dey T, Lee K, Kim D, Fabry B, Schmuki P. 2010. Size-selective separation of macromolecules by nanochannel titania membrane with self-cleaning (declogging) ability. *J. Am. Chem. Soc.* 132:7893–95
129. Song YY, Schmidt-Stein F, Berger S, Schmuki P. 2010. TiO_2 nano test tubes as a self-cleaning platform for high-sensitivity immunoassays. *Small* 6:1180–84
130. Joo J, Lee D, Yoo M, Jeon S. 2009. ZnO nanorod-coated quartz crystals as self-cleaning thiol sensors for natural gas fuel cells. *Sens. Actuator B-Chem.* 138:485–90
131. Yuan LY, Dai JJ, Fan XH, Song T, Tao YT, et al. 2011. Self-cleaning flexible infrared nanosensor based on carbon nanoparticles. *ACS Nano* 5:4007–13
132. Gant RM, Abraham AA, Hou Y, Cummins BM, Grunlan MA, Coté GL. 2010. Design of a self-cleaning thermoresponsive nanocomposite hydrogel membrane for implantable biosensors. *Acta Biomater.* 6:2903–10
133. Chen W, Qu L, Chang D, Dai L, Ganguli S, Roy A. 2008. Vertically-aligned carbon nanotubes infiltrated with temperature-responsive polymers: smart nanocomposite films for self-cleaning and controlled release. *Chem. Commun.* 2008:163–65
134. Janout V, Myers SB, Register RA, Regen SL. 2007. Self-cleaning resins. *J. Am. Chem. Soc.* 129:5756–59
135. Choi SJ, Huh SY. 2010. Direct structuring of a biomimetic anti-reflective, self-cleaning surface for light harvesting in organic solar cells. *Macromol. Rapid Commun.* 31:539–44
136. Park YB, Im H, Im M, Choi YK. 2011. Self-cleaning effect of highly water-repellent microshell structures for solar cell applications. *J. Mater. Chem.* 21:633–36
137. Zhu J, Hsu CM, Yu ZF, Fan SH, Cui Y. 2010. Nanodome solar cells with efficient light management and self-cleaning. *Nano Lett.* 10:1979–84
138. Tung WS, Daoud WA. 2011. Self-cleaning fibers via nanotechnology: a virtual reality. *J. Mater. Chem.* 21:7858–69
139. Abidi N, Cabrales L, Hequet E. 2009. Functionalization of a cotton fabric surface with titania nanosols: applications for self-cleaning and UV-protection properties. *ACS Appl. Mater. Interfaces* 1:2141–46
140. Bedford NM, Steckl AJ. 2010. Photocatalytic self cleaning textile fibers by coaxial electrospinning. *ACS Appl. Mater. Interfaces* 2:2448–55
141. Wang RH, Wang XW, Xin JH. 2010. Advanced visible-light-driven self-cleaning cotton by $Au/TiO_2/SiO_2$ photocatalysts. *ACS Appl. Mater. Interfaces* 2:82–85
142. Yuranova T, Laub D, Kiwi J. 2007. Synthesis, activity, and characterization of textiles showing self-cleaning activity under daylight irradiation. *Catal. Today* 122:109–17
143. Ramaratnam K, Tsyalkovsky V, Klep V, Luzinov I. 2007. Ultrahydrophobic textile surface via decorating fibers with monolayer of reactive nanoparticles and non-fluorinated polymer. *Chem. Commun.* 2007:451012
144. Editorial. 2005. A Chinese nano-society? *Nat. Mater.* 4:355
145. Sato O, Kubo S, Gu ZZ. 2009. Structural color films with lotus effects, superhydrophilicity, and tunable stop-bands. *Acc. Chem. Res.* 42:1–10
146. Markowska-Szczupak A, Ulfig K, Morawski AW. 2011. The application of titanium dioxide for deactivation of bioparticulates: an overview. *Catal. Today* 169:249–57
147. Dunnill CW, Aiken ZA, Kafizas A, Pratten J, Wilson M, et al. 2009. White light induced photocatalytic activity of sulfur-doped TiO_2 thin films and their potential for antibacterial application. *J. Mater. Chem.* 19:8747–54
148. Cao HQ, Zheng H, Yin JF, Lu YX, Wu SS, et al. 2010. $Mg(OH)_2$ complex nanostructures with superhydrophobicity and flame retardant effects. *J. Phys. Chem. C* 114:17362–68
149. Bormashenko E, Bormashenko Y. 2011. Non-stick droplet surgery with a superhydrophobic scalpel. *Langmuir* 27:3266–70
150. Das A, Megaridis CM, Liu L, Wang T, Biswas A. 2011. Design and synthesis of superhydrophobic carbon nanofiber composite coatings for terahertz frequency shielding and attenuation. *Appl. Phys. Lett.* 98:174101
151. Yang Y, Li JX, Wang H, Song XK, Wang TH, et al. 2011. An electrocatalytic membrane reactor with self-cleaning function for industrial wastewater treatment. *Angew. Chem. Int. Ed.* 50:2148–50

152. Faustini M, Nicole L, Boissière C, Innocenzi P, Sanchez C, Grosso D. 2010. Hydrophobic, antireflective, self-cleaning, and antifogging sol-gel coatings: an example of multifunctional nanostructured materials for photovoltaic cells. *Chem. Mater.* 22:4406–13
153. Liu K, Jiang L. 2011. Multifunctional integration: from biological to bio-inspired materials. *ACS Nano* 5:6786–90
154. Wong T-S, Kang SH, Tang SKY, Smythe EJ, Hatton BD, et al. 2011. Bioinspired self-repairing slippery surfaces with pressure-stable omniphobicity. *Nature* 477:443–47

Annual Review of
Materials Research

Volume 42, 2012

Contents

Index

Errata

An online log of corrections to *Annual Review of Materials Research* articles may be found at http://matsci.annualreviews.org/errata.shtml